Search for dark matter produced in association with a Higgs boson decaying to bottom quarks in proton-proton collisions at $\sqrt{s} = 13$ TeV

A. Hayrapetyan *et al.*[*]
(CMS Collaboration)

(Received 16 January 2026; accepted 13 March 2026; published 26 May 2026)

A search for dark matter particles produced in association with a Higgs boson decaying to a bottom quark-antiquark pair in proton-proton collisions at $\sqrt{s} = 13$ TeV is presented. The data, collected with the CMS detector at the LHC, correspond to an integrated luminosity of 101 fb^{-1}. The analysis is performed in exclusive categories targeting both Lorentz-boosted (merged) and resolved b jet pair topologies, covering a wide range of Higgs boson transverse momentum. A statistical combination is made with a previous search using data collected in 2016 and corresponding to an integrated luminosity of 35.9 fb^{-1}. The observed data agree with the standard model background predictions. Constraints are placed on models predicting new particles or interactions, such as those in the simplified frameworks of baryonic-Z' and 2HDM + a, where the latter is a type-II two-Higgs-doublet model featuring a heavy pseudoscalar with an additional light pseudoscalar. Upper limits at 95% confidence level are set on the production cross section for these models. For the baryonic-Z' model, Z' boson masses below 2.25 TeV are excluded for a dark matter particle candidate mass of 1 GeV. In the 2HDM + a model, heavy pseudoscalar masses between 850 and 1300 GeV are excluded for a light pseudoscalar mass of 350 GeV.

DOI: 10.1103/2m87-3dlr

I. INTRODUCTION

Strong astrophysical evidence supports the existence of dark matter (DM), providing compelling motivation for physics beyond the standard model (SM). Cosmological observations indicate that DM constitutes approximately 85% of the matter content in the Universe [1]. Since the existing evidence is based only on its gravitational interaction, whether DM interacts with the SM particles remains an open question. Many beyond the SM theories suggest a particle nature of DM [2], proposing several particle candidates that are compatible with the observed relic density of DM in the Universe [3]. The hypothesis that DM consists of stable or long-lived weakly interacting massive particles [4,5] drives many of the experimental searches at the CERN LHC.

A DM particle, if produced in high-energy proton-proton (pp) collisions at the LHC, can exit the detector undetected, becoming a source of large missing transverse momentum ($p_{\mathrm{T}}^{\mathrm{miss}}$). The presence of such a weakly interacting particle can be inferred if it is produced in association with a visible SM particle X (quark, gluon, photon, or heavy boson). Such an interaction may result in a "mono-X" signature with an SM particle or jet recoiling against $p_{\mathrm{T}}^{\mathrm{miss}}$. The SM particle X could be emitted directly from a parton as initial-state radiation or from a DM particle via a new coupling to SM particles.

The discovery of the SM Higgs (h) boson [6–8] allows the additional possibility of probing DM in the mono-Higgs channel [9,10], complementing other mono-X searches. The production of a Higgs boson from initial-state radiation is highly suppressed because of the mass dependence of its coupling strength to fermions and its loop-suppressed coupling to gluons [9–11]. The associated production of DM with a Higgs boson could therefore directly probe the structure of the effective DM-SM coupling [9]. In addition, there exist models where the coupling between the new physics sector and the Higgs boson is enhanced [12,13] or where the DM particles interact with the SM particles exclusively through the Higgs sector [14]. Owing to these features, the mono-Higgs channel offers a promising signature for the search for DM.

This analysis considers two simplified benchmark models for DM + Higgs boson production [15,16]. Figure 1 shows representative Feynman diagrams corresponding to these models.

In the baryonic-Z' model [9], the Z' particle is a vector boson mediator corresponding to a new baryon number symmetry, $U(1)_{\mathrm{B}}$. It radiates an h boson before decaying to a pair of Dirac fermions, $\chi\bar{\chi}$, which serve as DM candidates. The strength of the coupling between the h and Z' bosons is

[*]Full author list given at the end of the article.

Published by the American Physical Society under the terms of the Creative Commons Attribution 4.0 International license. Further distribution of this work must maintain attribution to the author(s) and the published article's title, journal citation, and DOI. Funded by SCOAP[3].

 © 2026 CERN, for the CMS Collaboration

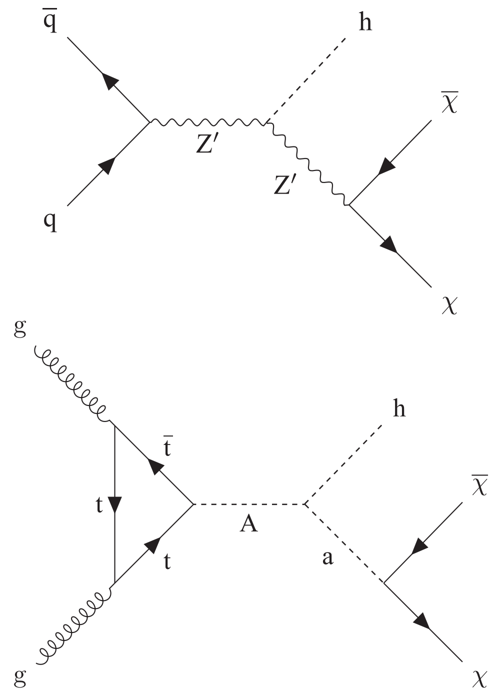

FIG. 1. Feynman diagrams for simplified benchmark models considered in this analysis: the baryonic-Z' model (left) and 2HDM + a model (right) [15,16].

assumed to be directly proportional to the mediator mass $m_{Z'}$. The coupling strengths of the Z' boson are chosen following Refs. [15,16], with the coupling between the Z' boson and DM particles, $g_\chi = 1$, and between the Z' boson and quarks, $g_q = 0.25$. The shape of the p_T^{miss} distribution depends mainly on two parameters, $m_{Z'}$ and the mass of the DM candidate m_χ, which are free parameters in the model and are varied in this search. This paper considers $m_{Z'}$ between 100 and 3500 GeV, and m_χ between 1 and 800 GeV.

The 2HDM + a model [17] is an extension of the type-II two-Higgs-doublet model [18], introducing an additional light pseudoscalar boson, a. The model predicts six mass eigenstates: the light scalar Higgs boson (h, mass m_h), the heavy scalar Higgs boson (H, mass m_H), the light pseudoscalar (a, mass m_a), the heavy pseudoscalar (A, mass m_A), and two heavy charged scalars ($H^\pm$, mass $m_{H^\pm}$). The states h and H are linear combinations of the CP-even weak eigenstates with mixing angle α, while the a and A states are linear combinations of the CP-odd weak eigenstates with mixing angle θ. The ratio of the vacuum expectation values of the two Higgs doublets is $\tan\beta$. The a boson decays to a pair of Dirac fermions, $\chi\bar{\chi}$. The model also includes three quartic couplings: λ_3, λ_{P_1}, and λ_{P_2}. Constraints from perturbativity and unitarity restrict their magnitude and sign, and benchmark values are chosen as $\lambda_3 = \lambda_{P_1} = \lambda_{P_2} = 3$ [15–17]. The parameter scans and fixed values are described in Sec. VII B. An important advantage of the 2HDM + a framework over simpler models is its rich phenomenology, which can yield complementary exclusion limits from different experimental searches.

This paper presents a search for DM produced in association with a Higgs boson decaying to a bottom quark-antiquark pair ($b\bar{b}$). This $b\bar{b}$ decay mode has the largest branching fraction and provides the highest signal yield among possible decay channels. A previous search in the same final state by the CMS experiment [19] was based on data collected in 2016 at a center-of-mass energy $\sqrt{s} = 13$ TeV with an integrated luminosity of 35.9 fb^{-1}. A similar search has been published by the ATLAS experiment at $\sqrt{s} = 13$ TeV corresponding to an integrated luminosity of 139 fb^{-1} [20]. No significant excess of events over the SM prediction was observed in either study.

The final state for this analysis, mono-$h(b\bar{b})$, is characterized by the presence of high p_T^{miss} and a Higgs boson decaying to a $b\bar{b}$ pair. The analysis is broadly categorized into merged and resolved categories, based on the transverse momentum of the reconstructed h boson candidate, p_T^h. Events with large p_T^h are assigned to the merged category, while those with relatively low to moderate p_T^h are included in the resolved category.

Compared to Ref. [19], we have nearly tripled the amount of data analyzed and enhanced the analysis sensitivity by means of improved identification of $h \to b\bar{b}$ decays. While such decays were previously selected using N-subjettiness [21], we now use criteria based on a deep neural network (DNN), resulting in increased sensitivity to the merged signals. We have further extended the sensitivity by combining the new results with the 2016 results, yielding a total data set of 138 fb^{-1}, equivalent in size to that of Ref. [20].

This paper is organized as follows. Section II provides a brief introduction to the CMS detector. Section III describes the data and simulation samples used. Section IV discusses the event reconstruction and various object definitions used in the search. The event selection, background estimation, and signal extraction procedures are detailed in Sec. V. Systematic uncertainties, both experimental and theoretical, are discussed in Sec. VI. The results are presented in Sec. VII, and a summary is given in Sec. VIII. Tabulated results are provided in the HEPData record for this analysis [22].

II. THE CMS DETECTOR

The central feature of the CMS apparatus is a superconducting solenoid with internal diameter of 6 m, providing a magnetic field of 3.8 T. Within the solenoid volume are a silicon pixel and strip tracker, a lead tungstate crystal electromagnetic calorimeter (ECAL), and a brass and scintillator hadron calorimeter (HCAL), each composed of a barrel and two end cap sections. Forward calorimeters extend the pseudorapidity (η) coverage provided by the barrel and end cap detectors. Muons are reconstructed in gas-ionization detectors embedded in the steel flux-return yoke outside the solenoid. More detailed descriptions of the CMS detector, together with a definition of the coordinate system used and the relevant kinematic variables, can be found in Refs. [23,24].

Events of interest are selected using a two-tiered trigger system. The first level (L1), composed of custom hardware processors, uses information from the calorimeters and muon detectors to select events at a rate of around 100 kHz within a fixed latency of 4 μs [25]. The second level, known as the high-level trigger (HLT), consists of a farm of processors running a version of the full event reconstruction software optimized for fast processing, and reduces the event rate to around 1 kHz before data storage [26].

III. DATA AND SIMULATED SAMPLES

The data analyzed in this search are from pp collisions at $\sqrt{s} = 13$ TeV collected by the CMS experiment in 2017 and 2018, corresponding to an integrated luminosity of 101 fb^{-1}. Signal and background contributions are modeled using Monte Carlo (MC) simulations. All samples use NNPDF3.1 parton distribution functions (PDFs) at next-to-next-to-leading order accuracy [27,28]. The parton shower, hadronization, and the underlying event simulation are provided by PYTHIA [29] version 8.202 or later with the underlying event tune CP5 [30]. The response of the CMS detector is simulated with the Geant4 package [31]. Simulated events are reconstructed with the same software as used for data events. All samples include the effects of additional pp interactions within the same or nearby bunch crossings (pileup). Minimum bias interactions simulated with PYTHIA are overlaid on the hard scattering interaction with a multiplicity distribution matching that observed in the collider data.

For both the simplified DM models considered, baryonic-Z' and $2\mathrm{HDM} + a$, the signal samples are generated at leading order (LO) using MadGraph5_aMC@NLO [32] version 2.6.5. The dominant background arises from the production of $Z(\nu\nu) + \mathrm{jets}$ and $t\bar{t}$ pairs. The $Z(\nu\nu) + \mathrm{jets}$ process is generated using MadGraph5_aMC@NLO at next-to-LO (NLO) precision in perturbative quantum chromodynamics (pQCD). The lepton + jets decay of the $t\bar{t}$ pair constitutes the leading background contribution compared to dileptonic or hadronic decays. All three $t\bar{t}$ decay modes are simulated at NLO in pQCD using the POWHEGv2.0 generator [33–35]. The p_{T} spectra of top quarks in $t\bar{t}$ data have been observed to be significantly softer compared to MC simulations at LO or NLO, attributed to missing higher-order calculations. To mitigate this discrepancy, $t\bar{t}$ events in simulation are reweighted using a parametric function [36].

Subleading contributions arise from $W + \mathrm{jets}$, single top quark, and diboson (WW, WZ, and ZZ) processes. The $W + \mathrm{jets}$ background contributes to this analysis when the lepton is not reconstructed or identified, or falls outside the detector acceptance. Events from $W + \mathrm{jets}$ and $Z(\ell\ell) + \mathrm{jets}$ processes are simulated using the MadGraph5_aMC@NLO generator at LO, and the cross section is scaled to NLO accuracy in pQCD and electroweak (EW) corrections. Event generation for the production of a single top quark in the t channel [37] and in association with a W boson [38] is performed at NLO with the POWHEG generator. Diboson background events are simulated at NLO in pQCD with the POWHEG or MadGraph5_aMC@NLO generator.

The SM backgrounds with genuine Higgs bosons are produced via different processes: gluon-gluon fusion, vector boson fusion, in association with a vector boson, or in association with a pair of top quarks. These SM Higgs boson samples are all generated with POWHEG at NLO in pQCD. The background from SM events composed uniquely of jets produced through the strong interaction, referred to as QCD multijet events, is also considered. These are generated at LO using MadGraph5_aMC@NLO.

The merging schemes employed for the MadGraph5_aMC@NLO LO and NLO samples with the parton shower model are MLM [39] and FxFx [40], respectively.

IV. EVENT RECONSTRUCTION

The CMS particle-flow (PF) algorithm [41] aims to reconstruct and identify each individual particle in an event, with an optimized combination of information from the various elements of the CMS detector. The energy of photons is obtained from the ECAL measurement. The energy of electrons is determined from a combination of the electron momentum at the primary interaction vertex as determined by the tracker, the energy of the corresponding ECAL cluster, and the energy sum of all bremsstrahlung photons spatially compatible with originating from the electron track. The energy of muons is obtained from the curvature of the corresponding track. The energy of charged hadrons is determined from a combination of their momentum measured in the tracker and the matching ECAL and HCAL energy deposits, corrected for the response function of the calorimeters to hadronic showers. Finally, the energy of neutral hadrons is obtained from the corresponding corrected ECAL and HCAL energies.

The primary vertex (PV) is taken to be the vertex corresponding to the hardest scattering in the event, evaluated using tracking information alone, as described in Section 9.4.1 of Ref. [42].

The electron momentum is estimated by combining the energy measurement in the ECAL with the momentum measurement in the tracker [43,44]. The momentum resolution for electrons with $p_{\mathrm{T}} \approx 45$ GeV from $Z \to ee$ decays ranges from 1.6 to 5%. A multivariate approach is used to identify prompt electrons arising from the decays of W or Z bosons. Two identification criteria, corresponding to the expected electron identification efficiency of either 90% (loose working point, WP) or 80% (tight WP), are used in this analysis. The loose WP is used for rejecting events for the 0-lepton signal region (SR), as well as for rejecting events containing extra electrons for the single or dimuon control regions (CRs). The tight WP is used to select events in the single or dielectron control regions. The electron p_{T} threshold required for the loose (tight) selection is 10 (35) GeV.

Muons are measured in the pseudorapidity range $|\eta| < 2.4$, with detection planes made using three technologies: drift tubes, cathode strip chambers, and resistive plate chambers. The single muon trigger efficiency exceeds 90% over the full η range, and the efficiency to reconstruct and identify muons is greater than 96%. Matching muons to tracks measured in the silicon tracker results in a relative transverse momentum resolution, for muons with p_{T} up to 100 GeV, of 1% in the barrel and 3% in the end caps. In the central region of the detector, the p_{T} resolution is better than 7% for muons with p_{T} up to 1 TeV [45]. Two sets of selection conditions, corresponding to 96–98% (tight WP) and ~99% (loose WP) efficiency for the identification of prompt muons, are used in the analysis. The use of loose and tight WPs across different analysis regions is similar to the approach used for electrons. The muon p_{T} threshold for the loose (tight) selection is 15 (30) GeV.

The contribution of misidentified electrons or muons is further reduced by requiring the lepton candidate to satisfy isolation criteria that limit the total energy of tracks and calorimeter clusters measured in conical regions around them.

Hadronic τ decays (τ_{h}) are reconstructed from jets using the hadrons-plus-strips algorithm [46], which combines 1 or 3 tracks with energy deposits in the calorimeters to identify the tau decay modes. To distinguish genuine τ_{h} decays from jets originating from the hadronization of quarks or gluons, and from electrons or muons, a convolutional discriminator based on a DNN called DeepTau [47] is used. Information from all individual reconstructed particles near the τ_{h} axis is combined with properties of the τ_{h} candidate and the event. The rate of a jet to be misidentified as τ_{h} by the DeepTau algorithm depends on the p_{T} and quark flavor of the jet. In simulated events from W boson production in association with jets it has been estimated to be 0.43% for a genuine τ_{h} identification efficiency of 70%.

Jets are reconstructed from the PF particles using the infrared- and collinear-safe anti-k_{T} algorithm [48,49] with distance parameters 0.4 (“AK4 jets”) and 0.8 (“AK8 jets”). The distance parameter value 0.4 is found to optimize the reconstruction of jets initiated by a single quark or gluon. For the boosted topology in this analysis, the two h-daughter b jets have angular separation too small to be resolved, but are captured in a single wider jet reconstructed by setting the algorithm’s distance parameter to 0.8. Jet momentum is determined as the vectorial sum of all particle momenta in the jet, and is found from simulation to be, on average, within 5 to 10% of the momentum at particle level over the entire p_{T} spectrum and detector acceptance.

The pileup-per-particle identification algorithm [50,51] is used to mitigate the effect of pileup at the reconstructed particle level, making use of local shape information, event pileup properties, and tracking information. Charged particles identified to be originating from pileup vertices are discarded. For each neutral particle, a local shape variable is computed using the surrounding charged particles compatible with the PV within the tracker acceptance, and using both charged and neutral particles in the region outside of the tracker coverage. The momenta of the neutral particles are then rescaled according to their probability to originate from the PV deduced from the local shape variable, superseding the need for jet-based pileup corrections [50].

Jet energy corrections are derived from simulation studies so that the average measured energy of jets becomes consistent with that of particle-level jets within uncertainties. *In situ* measurements of the momentum balance in dijet, photon + jet, Z + jet, and multijet events are used to determine any residual differences between the jet energy scale (JES) and jet energy resolution (JER) in data and in simulation, and appropriate corrections are made [52,53]. The JER amounts typically to 15–20% at 30 GeV, 10% at 100 GeV, and 5% at 1 TeV [52]. Additional selection criteria are applied to each jet to remove jets potentially stemming from instrumental effects or reconstruction failures [50]. Jets overlapping with the selected electrons and muons (i.e., those with $\Delta R < 0.4$ for $\Delta R = \sqrt{(\Delta\eta)^2 + (\Delta\phi)^2}$ for AK4 jets, and $\Delta R < 0.8$ for AK8 jets) are removed. Only jets within the tracker volume, with $|\eta| < 2.5$, are considered in the analysis.

The missing transverse momentum vector $\vec{p}_{\mathrm{T}}^{\,\mathrm{miss}}$ is computed as the negative vector sum of the transverse momenta of all the PF candidates in an event, and its magnitude is denoted as $p_{\mathrm{T}}^{\mathrm{miss}}$ [54]. The $\vec{p}_{\mathrm{T}}^{\,\mathrm{miss}}$ is modified to account for corrections to the JES and JER of the reconstructed jets in the event. Anomalous high-$p_{\mathrm{T}}^{\mathrm{miss}}$ events can arise from a variety of reconstruction failures, detector malfunctions or noncollision backgrounds. Such events are rejected by event filters that are designed to identify more than 85–90% of the spurious high-$p_{\mathrm{T}}^{\mathrm{miss}}$ events with a false positive rate below 0.1% [54].

Large-radius AK8 jets are used to identify the Lorentz-boosted hadronically decaying Higgs bosons. For these jets, a grooming algorithm is used, where the constituents of the AK8 jet are reclustered using the Cambridge-Aachen algorithm [55,56]. The “modified mass drop tagger” algorithm [57,58], also known as the “soft-drop” algorithm [59], with angular exponent $\beta = 0$, soft cutoff threshold $z_{\mathrm{cut}} < 0.1$, and characteristic radius $R_0 = 0.8$, is applied to remove soft, wide-angle radiation from the jet, mitigating pileup and underlying event contamination to improve the mass resolution and enhance the identification of boosted, hadronically decaying Higgs bosons.

The AK4 b jet identification is performed using the DeepJet algorithm [60,61], a DNN-based tagger that utilizes information from charged and neutral particles, as well as secondary vertices within a jet, to determine the likelihood that the jet originates from a bottom quark. For an AK4 jet to be tagged as a bottom jet, its DeepJet b tagging discriminator score is required to be larger than a specific threshold. The threshold values, corresponding to false positive rates for jets initiated by light quarks or gluons of 10, 1, and 0.1%, are referred to as loose, medium, and tight WPs, respectively. In the resolved category, to identify the b jets originating from the Higgs boson decay, a medium WP is used, which has a signal efficiency of 80%. In the merged category, to identify and veto AK4 b jets away from the Higgs boson candidate AK8 jet, a loose WP for the DeepJet tagger with signal efficiency of 90% is used. To match the efficiency of b tagging in data, correction factors are applied to simulated events as a function of jet p_{T}, η, and the flavor of the initiating parton. The performance of the DeepJet tagger and its calibration results using 2016–2018 data are summarized in Ref. [62].

To identify AK8 jets originating from the $h \to b\bar{b}$ decay, a dynamic graph convolutional neural-network-based tagger, ParticleNet [63] with its mass decorrelated version (ParticleNet-MD), is used. The algorithm is trained to identify two-prong hadronic decays of Lorentz-boosted heavy particles, and the tagger performance is decorrelated from the mass of the parent particle, which allows it to be used in various analyses with a wide range of resonance masses. It uses jet constituents and secondary vertices associated with the jet, with the tagger score specifying the likelihood that the jet originates from a heavy particle decaying to a b quark-antiquark pair $X \to b\bar{b}$, as compared to light quarks or gluons. The loose WP threshold is used, such that the discriminator score is chosen to achieve a signal efficiency of 80% and a misidentification rate of 1% for light quark or gluon jets. Calibration is performed [64] using an event sample in data enriched in jets originating from $g \to b\bar{b}$ splittings, which have a similar substructure as $h \to b\bar{b}$ decay. Correction factors are applied in simulation, parametrized as functions of the AK8 jet p_{T}, to match the efficiency of b tagging in data, with a performance summarized in Ref. [65].

A section of the HCAL was not operational during a portion of the 2018 data-taking period, which affected approximately 65% of the total integrated luminosity collected in 2018. This resulted in irrecoverable energy mismeasurements in a localized region of the detector, defined by $-1.57 < \phi < -0.87$ and $-3.0 < \eta < -1.3$. To mitigate the impact of these mismeasurements, events are vetoed if any AK4 jet with $p_{\mathrm{T}} > 30$ GeV, or any AK8 jet with $p_{\mathrm{T}} > 200$ GeV, is found within the affected region in the 2018 data set. Additionally, in the electron control regions, events are rejected if any electron with $p_{\mathrm{T}} > 30$ GeV is present in the affected region. Events with severe mismeasurement, where a jet is fully lost in the affected HCAL region, are found to contribute predominantly at low $p_{\mathrm{T}}^{\mathrm{miss}}$ (<470 GeV) and exhibit a characteristic $\phi(\vec{p}_{\mathrm{T}}^{\mathrm{miss}})$ distribution. To veto such events, an additional selection is applied: events with $p_{\mathrm{T}}^{\mathrm{miss}} < 470$ GeV are rejected if $-1.62 < \phi(\vec{p}_{\mathrm{T}}^{\mathrm{miss}}) < -0.62$. The threshold of 470 GeV is chosen to efficiently remove the majority of these background events, while maintaining high signal efficiency.

V. EVENT SELECTION

In the boosted regime, the $h \to b\bar{b}$ decay products are highly collimated and reconstructed as an AK8 jet. For low to moderate p_{T}^{h} with well-separated decay products, AK4 jets are used to reconstruct particles from the b quark fragmentation.

The two categories are orthogonal by construction. Events are first considered for the merged category, and those failing this selection are passed on to the selection criteria for the resolved category. This helps improve the overall sensitivity of the analysis to different regions of parameter space.

Events with any loosely reconstructed tau lepton candidate with $p_{\mathrm{T}} > 20$ GeV, $|\eta| < 2.3$ and $|d_z| < 0.2$ cm are vetoed in all analysis regions, where d_z is the longitudinal impact parameter. Events containing an isolated photon candidate with $p_{\mathrm{T}} > 20$ GeV, $|\eta| < 2.5$, and passing loose identification criteria with 90% efficiency, are also vetoed in all analysis regions.

A. Signal region

The events in the signal region are selected using a trigger with a $p_{\mathrm{T}}^{\mathrm{miss}}$ threshold of 120 GeV, where the calculation of $p_{\mathrm{T}}^{\mathrm{miss}}$ is based on all PF candidates reconstructed at the HLT. The p_{T} of muon candidates identified by the PF algorithm is subtracted in this calculation. As a result, events with high-p_{T} muons are associated with large $p_{\mathrm{T}}^{\mathrm{miss}}$, which allows us to use the same trigger path to select events populating single-muon and dimuon control regions. The $p_{\mathrm{T}}^{\mathrm{miss}}$ trigger efficiency is around 90% for $p_{\mathrm{T}}^{\mathrm{miss}} = 200$ GeV and reaches 99% for 300 GeV and above. Events in the SR are required to have $p_{\mathrm{T}}^{\mathrm{miss}} > 250$ (200) GeV in the merged (resolved) category.

To reduce the $t\bar{t}$ and $W +$ jets background contribution in the SRs, events are required to have no isolated electron (muon) with $p_{\mathrm{T}} > 10$ (15) GeV and $|\eta| < 2.5$ (2.4) that passes loose quality criteria. The symbol ℓ denotes either an electron or muon, and N_{ℓ} the number of electrons or muons in an event.

In the merged-category SR, exactly one AK8 jet ($N_{\mathrm{AK8}} = 1$) is required with $p_{\mathrm{T}} > 200$ GeV, $|\eta| < 2.5$, and soft-drop-corrected mass (m_{SD}) within $70 < m_{\mathrm{SD}} < 160$ GeV, a window around the h boson mass that includes sidebands for the evaluation of background. To select events where the AK8 jet originates from an $h \to b\bar{b}$

TABLE I. Event selections applied to the merged-category SR and CRs. Events in all the analysis regions have a photon and tau lepton candidate veto. Here "jets" refers to the AK4 jets with $\Delta R > 0.8$ between the jet and the double-b tagged AK8 jet.

	Merged category selection		
Variable	SR	$t(\ell)$ CR	$Z(\ell\ell)$ CR
p_T^{miss} (GeV)	>250	>50	…
U (GeV)	…	>250	>250
$N_{AK8\,jets}$	1 [$p_T > 200$ GeV, $70 < m_{SD} < 160$ GeV, double-b tagged]	1 [$p_T > 200$ GeV, $70 < m_{SD} < 160$ GeV, double-b tagged]	1 [$p_T > 200$ GeV, $70 < m_{SD} < 160$ GeV]
N_{jets}	≤2	≤2	≤2
N_{bjets}	0	1	0
N_{ℓ}	0	1	2
$p_T^{\ell\ell}$ (GeV)	…	…	>200
$m_{\ell\ell}$ (GeV)	…	…	∈ [60–120]
$\Delta\phi(\vec{p}_T^{miss}, \vec{p}_T^{jet})$	>0.4	…	…
$\Delta\phi(\vec{p}_T^{miss}, \vec{p}_T^{AK8})$	>0.8	…	…
$\Delta\phi(\mathrm{PF}\vec{p}_T^{miss}, \mathrm{track}\vec{p}_T^{miss})$	<2.0	…	…

decay, the jet must pass the loose WP of the ParticleNet-MD double-b algorithm. Furthermore, to reduce the $t\bar{t}$ background contribution, a selection is placed on the number of AK4 jets, N_{jets}, where we allow up to two such jets with $p_T > 30$ GeV that do not overlap with the h candidate AK8 jet, i.e., $\Delta R > 0.8$. Events where the number of AK4 jets passing the loose DeepJet WP (N_{bjets}) is greater than zero are vetoed. These selection criteria are summarized in Table I, along with those of the CRs.

In the resolved-category SR, the two b-tagged AK4 jets must pass p_T thresholds of 50 and 30 GeV. To reduce the $t\bar{t}$ background by a factor of two while preserving high acceptance for signal events, the h candidate, i.e., the "dijet" system formed by the two b-tagged AK4 jets, must have transverse momentum $p_T^{b\bar{b}} > 100$ GeV and invariant mass ($m_{b\bar{b}}$) within 70–160 GeV. We impose a requirement similar to the one for the merged category to suppress the $t\bar{t}$ background: $N_{jets} \leq 2$, counting AK4 jets with $p_T > 30$ GeV within $\Delta R > 0.4$ of either b-tagged jet forming the h candidate. These selection criteria are summarized in Table II, along with those of the CRs. Figure 2 shows the AK8 jet m_{SD} distribution in the merged category (left) and the dijet $m_{b\bar{b}}$ distribution in the resolved category (right).

The QCD multijet events can mimic the signal-like final state with a large artificial p_T^{miss} arising from jet momentum mismeasurements or from failures in the PF reconstruction. In the first scenario, the events have a characteristic feature with small azimuthal angle difference between the misreconstructed jet $\vec{p}_T^{jet}$ and the $\vec{p}_T^{miss}$ vector. To ensure that a jet mismeasurement is not the cause of p_T^{miss}, the $\Delta\phi(\vec{p}_T^{miss}, \vec{p}_T^{jet})$ for AK4 jets is required to be larger than 0.4, which is the typical angular size of an AK4 jet. Additionally, in the merged category, requiring $\Delta\phi(\vec{p}_T^{miss}, \vec{p}_T^{AK8}) > 0.8$ between $\vec{p}_T^{miss}$ and the AK8 jet, as well as in the resolved category, requiring $\Delta\phi(\vec{p}_T^{miss}, \vec{p}_T^{b\bar{b}}) > 1.6$ between $\vec{p}_T^{miss}$ and the dijet system, reduces the QCD background contamination significantly. In the second scenario, the events in the SR are required to have a maximum azimuthal angular separation between the PF-based and charged-particle track-based $\vec{p}_T^{miss}$ of

TABLE II. Event selections applied to the resolved-category SR and CRs. Events in all the analysis regions have a photon and tau lepton candidate veto. Here jets refers to the AK4 jets with $\Delta R > 0.4$ between this jet and the leading (j_1) and subleading (j_2) b-tagged jets forming the Higgs boson candidate dijet (jj) system.

	Resolved category selection		
Variable	SR	$t(\ell)$ CR	$Z(\ell\ell)$ CR
p_T^{miss} (GeV)	>200	>50	< 100
U (GeV)	…	>200	>200
$p_T^{j_1}$, $p_T^{j_2}$ (GeV)	>50, >30 b-tagged	>50, >30 b-tagged	>50, >30 …
p_T^{jj} (GeV)	>100	>100	>100
m_{jj} (GeV)	∈ [70–160]	∈ [70–160]	∈ [70–160]
N_{jets}	≤2	≥1	≤2
N_{ℓ}	0	1	2
$p_T^{\ell\ell}$ (GeV)	…	…	>200
$m_{\ell\ell}$ (GeV)	…	…	∈ [60–120]
$\Delta\phi(\vec{p}_T^{miss}, \vec{p}_T^{jet})$	>0.4	…	…
$\Delta\phi(\vec{p}_T^{miss}, \vec{p}_T^{jj})$	>1.6	…	…
$\Delta\phi(\mathrm{PF}\,\vec{p}_T^{miss}, \mathrm{track}\,\vec{p}_T^{miss})$	<2.0	…	…

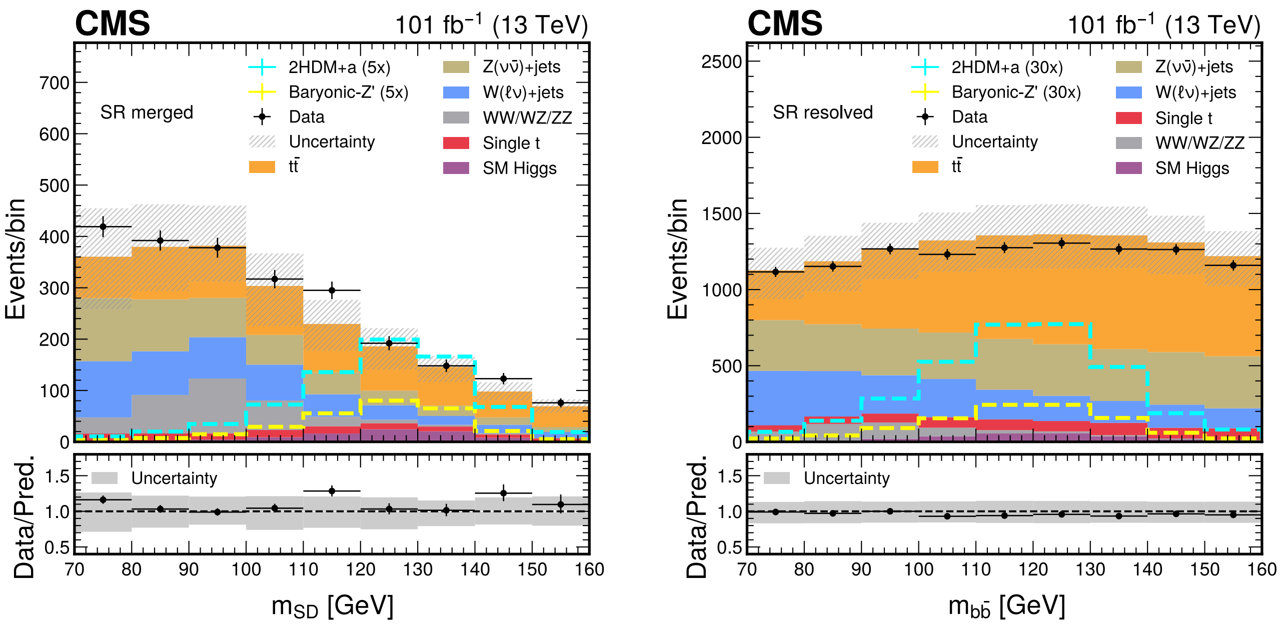

FIG. 2. Distributions in the AK8 jet soft-drop mass m_{SD} for the merged category (left), and in the dijet mass $m_{b\bar{b}}$ for the resolved category (right), SRs. The black markers with statistical uncertainty bars show the observed data, the stacked colored histograms show the predicted prefit background, and the gray shading shows the statistical uncertainty in the prediction. The signal predictions, scaled up for visibility by the factors indicated in the legends, are overlaid as yellow and cyan dashed lines, one for each benchmark model: baryonic-Z' with $(m_{Z'} = 2250, m_\chi = 1)$ GeV and 2HDM + a with $(m_A = 1000, m_a = 350)$ GeV, respectively. The lower panels show the ratios of the observed data to the predicted background, with the gray bands indicating the systematic uncertainty.

$\Delta\phi(\mathrm{PF}\,\vec{p}_{\mathrm{T}}^{\,\mathrm{miss}}, \mathrm{track}\,\vec{p}_{\mathrm{T}}^{\,\mathrm{miss}}) < 2$. The QCD multijet background passing these requirements is less than 1% of the total background.

B. Background estimation and control regions

The dominant background processes, $t\bar{t}$ and $Z(\nu\nu)$ + jets, are estimated separately in each SR category using dedicated CRs, as detailed in Sec. V C. Single-lepton CRs are used to estimate the $t\bar{t}$ contribution, of which the lepton plus jets decay is the most important, while dilepton CRs, enriched in $Z(\ell\ell)$ + jets events, are used to estimate the $Z(\nu\nu)$ + jets background. The CRs are built by requiring exactly one or two well-reconstructed electrons or muons that satisfy stringent quality criteria. These regions are illustrated in Fig. 3 with single-lepton CRs—referred to as $t(\ell)$ CRs—and dilepton CRs—referred to as $Z(\ell\ell)$ CRs—defined separately for each SR category.

Events in the electron CRs are selected using a single-electron trigger, with at least one electron with $p_{\mathrm{T}} > 32$ GeV. Events in the muon CRs are selected using the $p_{\mathrm{T}}^{\mathrm{miss}}$ trigger with a $p_{\mathrm{T}}^{\mathrm{miss}}$ threshold of 120 GeV, as discussed in Sec. V A.

The hadronic recoil $\vec{U}$ is defined by removing the electron(s) or muon(s) $\vec{p}_{\mathrm{T}}^{\,\ell}$ from the $\vec{p}_{\mathrm{T}}^{\,\mathrm{miss}}$ calculation in the CRs, and its magnitude U acts as a proxy for $p_{\mathrm{T}}^{\mathrm{miss}}$ in the SRs. Events in the CRs are required to have $U > 250$ GeV in the merged and $U > 200$ GeV in the resolved category.

In each of the CRs, a similar selection strategy as in the corresponding SR (merged or resolved) is imposed, except for the charged-lepton selection criterion. In the $t(\ell)$ CRs,

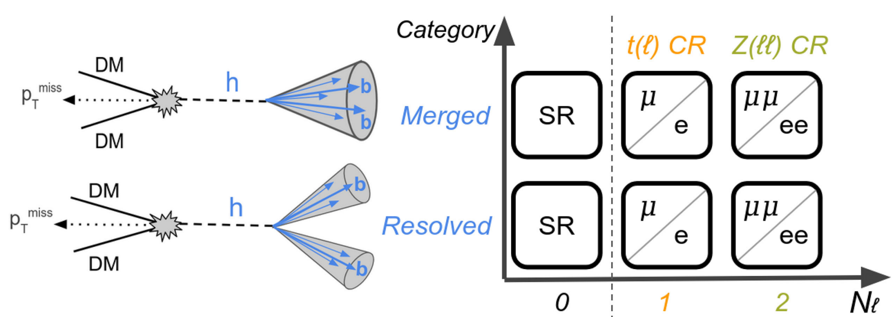

FIG. 3. Schematic representation of the analysis regions.

exactly one electron (muon) with $p_{\mathrm{T}} > 35$ (30) GeV is required that passes tight identification and isolation quality criteria, corresponding to an identification efficiency of 90 (95)%. In the $Z(\ell\ell)$ CRs, two oppositely charged electrons or muons are required that satisfy the same set of tight quality criteria. Furthermore, the dilepton p_{T} must be above 200 GeV with the dilepton invariant mass in the Z boson mass window, $60 < m_{\ell\ell} < 120$ GeV.

To accurately model the $Z(\nu\nu)+$jets background process in the SRs, a sufficient number of $Z(\ell\ell)+$jets events are retained in the $Z(\ell\ell)$ CRs by relaxing the b-tagging condition for the h candidate. In the merged category, the ParticleNet-MD double-b tagging requirement for the AK8 jet is dropped. Similarly, in the resolved category, we drop the DeepJet b tagging requirement for the AK4 jet candidates making up the h candidate dijet system.

In the $t(\ell)$ CR of the merged category, one of the b jets in $t\bar{t}$ events is captured by the AK8 jet identified with the ParticleNet-MD double-b algorithm. To capture the second b jet in a $t\bar{t}$ event, we require an additional b-tagged AK4 jet that is separated from the AK8 jet by $\Delta R > 0.8$. In the $t(\ell)$ CR of the resolved category, the presence of two AK4 b tagged jets is already accounted for.

Furthermore, in the $t(\ell)$ CRs, events are required to satisfy $p_{\mathrm{T}}^{\mathrm{miss}} > 50$ GeV to select events with the lepton + jets decay of the $t\bar{t}$ pair while suppressing other background contributions. For the $Z(\ell\ell)$ CRs, $p_{\mathrm{T}}^{\mathrm{miss}} < 100$ GeV is required to ensure a high purity of $Z(\ell\ell)+$jets events and to remain in a kinematic region where the modeling of $p_{\mathrm{T}}^{\mathrm{miss}}$ in simulation is well understood. Tables I and II summarize the merged and resolved event selections in the respective categories for the SRs and CRs.

C. Signal extraction

The analysis is performed in the merged and resolved categories using a two-dimensional maximum likelihood fit. The observables are $p_{\mathrm{T}}^{\mathrm{miss}}$ and the Higgs boson candidate mass m_{SD} in the merged category and $m_{b\bar{b}}$ in the resolved category. The Higgs boson candidate mass provides strong discrimination, as only the signal and well-understood, subdominant SM backgrounds exhibit a resonant peak in this distribution. The signal hypotheses typically exhibit harder $p_{\mathrm{T}}^{\mathrm{miss}}$ than the dominant SM backgrounds, leading to a progressively improved signal-to-background ratio at high $p_{\mathrm{T}}^{\mathrm{miss}}$. To enhance the sensitivity of the analysis, we slice into exclusive $p_{\mathrm{T}}^{\mathrm{miss}}$ regions and perform a simultaneous fit across all regions. A variable binning is used for $p_{\mathrm{T}}^{\mathrm{miss}}$ in SRs (U in CRs), which is optimized for signal sensitivity and tailored separately for each category. The bin edges are 250, 350, and 500 GeV for the merged category, and 200, 250, 290, 360, and 420 GeV for the resolved category. Thus, the signal is extracted using both the SRs and the corresponding CRs simultaneously in the binned maximum likelihood fit.

For the dominant backgrounds, $t\bar{t}$ and $Z(\nu\nu)+$jets, the Higgs boson candidate mass distribution in each $p_{\mathrm{T}}^{\mathrm{miss}}$ window of the SRs is tied to the corresponding U window in the CRs via a scale factor whose systematic uncertainty is accounted for with a nuisance parameter in the fit. For each category, the electron and muon CRs are combined appropriately to form a single CR for each background estimated from data. The contributions from other background processes are taken directly from MC simulation, with their nominal expected yield obtained after applying all event selections and normalizing them to the integrated luminosity times their respective theoretical cross sections.

The fit to the data determines the background postfit yields in each bin, which are obtained as the prefit yields adjusted by the postfit values of the scale factors through their associated nuisance parameters. The systematic uncertainties, many of which are shape based, account for experimental sources, such as jet energy scale and resolution, b tagging, lepton identification and trigger efficiencies, as well as theoretical uncertainties affecting the background and signal distributions, detailed in Sec. VI. The shape-based systematic uncertainties further ensure that any residual mismodeling is accounted for in the total uncertainty.

The final free parameter in the fit is the signal strength modifier μ, which controls the signal normalization relative to the theoretical cross section for a given signal hypothesis. The best fit background model, and the best fit signal strength are simultaneously obtained by maximizing the likelihood fit across the two categories, all SRs and CRs, and all data-taking periods.

Figures 4 and 5 show the postfit h candidate mass distributions in the merged-category $t(\ell)$ and $Z(\ell\ell)$ CRs, respectively, and Figs. 6 and 7 show the corresponding distributions for the resolved-category CRs. The lower panels display the ratio of the yields in data to the prediction before (prefit) and after (postfit) the fit. The agreement of these postfit yields with those observed in the data in the CRs provides additional confidence in the method.

VI. SYSTEMATIC UNCERTAINTIES

All systematic uncertainties affecting the simulated processes (signal and background) in the analysis regions are treated as nuisance parameters within the likelihood function. These parameters influence either the normalization or the shape of the $p_{\mathrm{T}}^{\mathrm{miss}}$ (U) distribution for a given process in the SR (CR) and are constrained in the simultaneous fit.

Uncertainties that do not affect the shape of the distribution, or are uniformly distributed are treated as normalization uncertainties and incorporated using log-normal distributions. Those having nonuniform variations are treated as shape uncertainties and are incorporated by means of Gaussian prior distributions. Experimental and

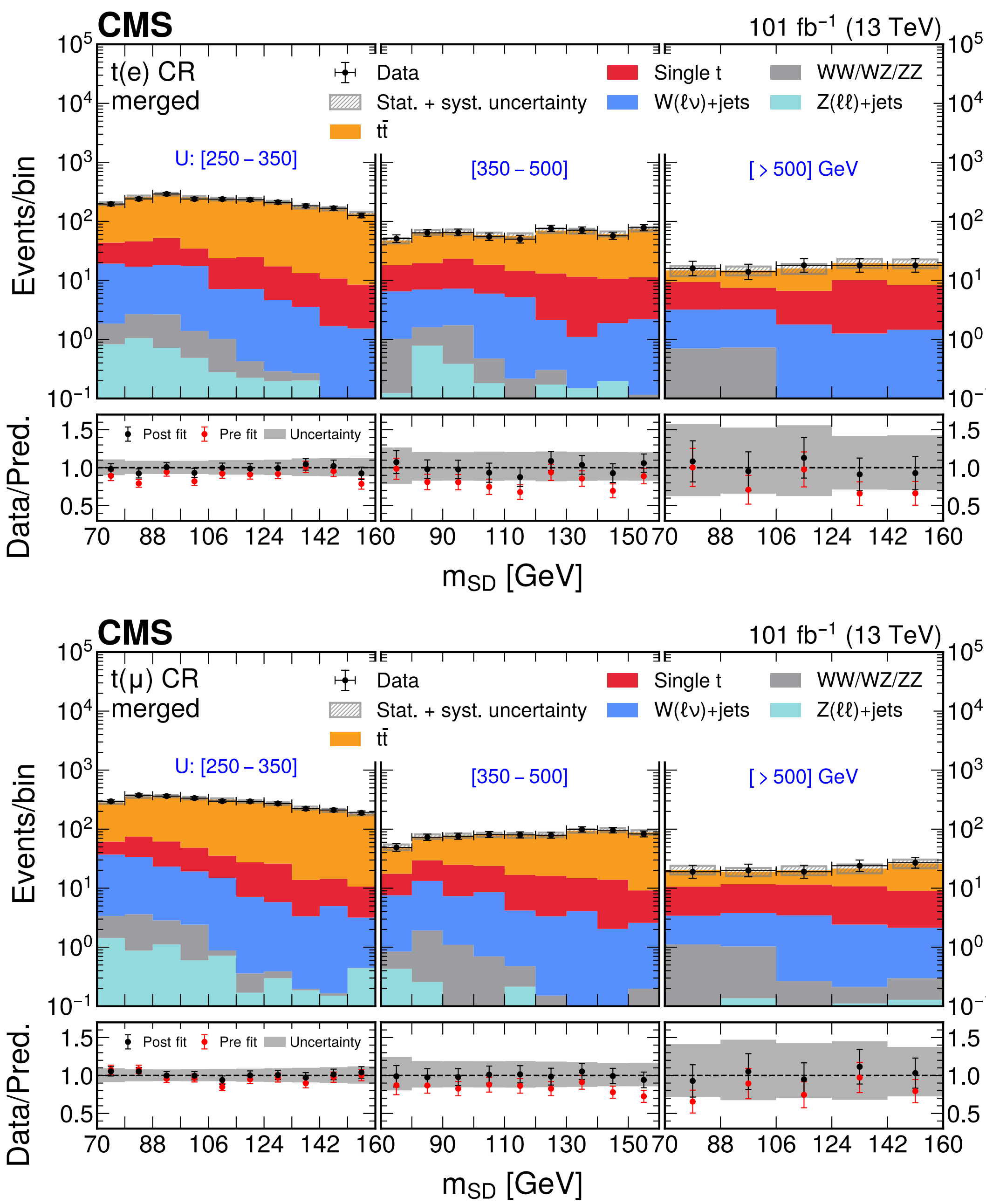

FIG. 4. The AK8 jet m_{SD} distributions after the simultaneous likelihood background-only fit sliced in three U bins, for the merged-category $t(e)$ (above) and $t(\mu)$ (below) CRs. The black markers with statistical uncertainty bars show the observed data, the stacked colored histograms show the predicted background, and the gray shading shows the systematic uncertainty in the prediction. The lower panels show the ratios of the observed data to the background predicted before (prefit in red) and after (postfit in black) the fit, with the gray bands indicating the postfit uncertainty obtained from combining all statistical and systematic sources.

theoretical sources of systematic uncertainty considered in this search are described below.

The $p_{\mathrm{T}}^{\mathrm{miss}}$ trigger efficiency is measured using single-muon events passing the single-muon trigger with a p_{T} threshold of 27 (24) GeV for data recorded in 2017 (2018). It is parametrized as a function of the U variable, and the corresponding data-to-simulation correction factors are applied to the simulation in the SRs and the single-muon and dimuon CRs. The electron trigger efficiency is parametrized as a function of the electron p_{T} and η. An associated uncertainty of 1–2% is assigned to both the trigger scale factors.

Lepton reconstruction and identification uncertainties are evaluated and incorporated as a function of p_{T} and η. The systematic uncertainties related to muon identification and isolation have a normalization effect of less than 1%.

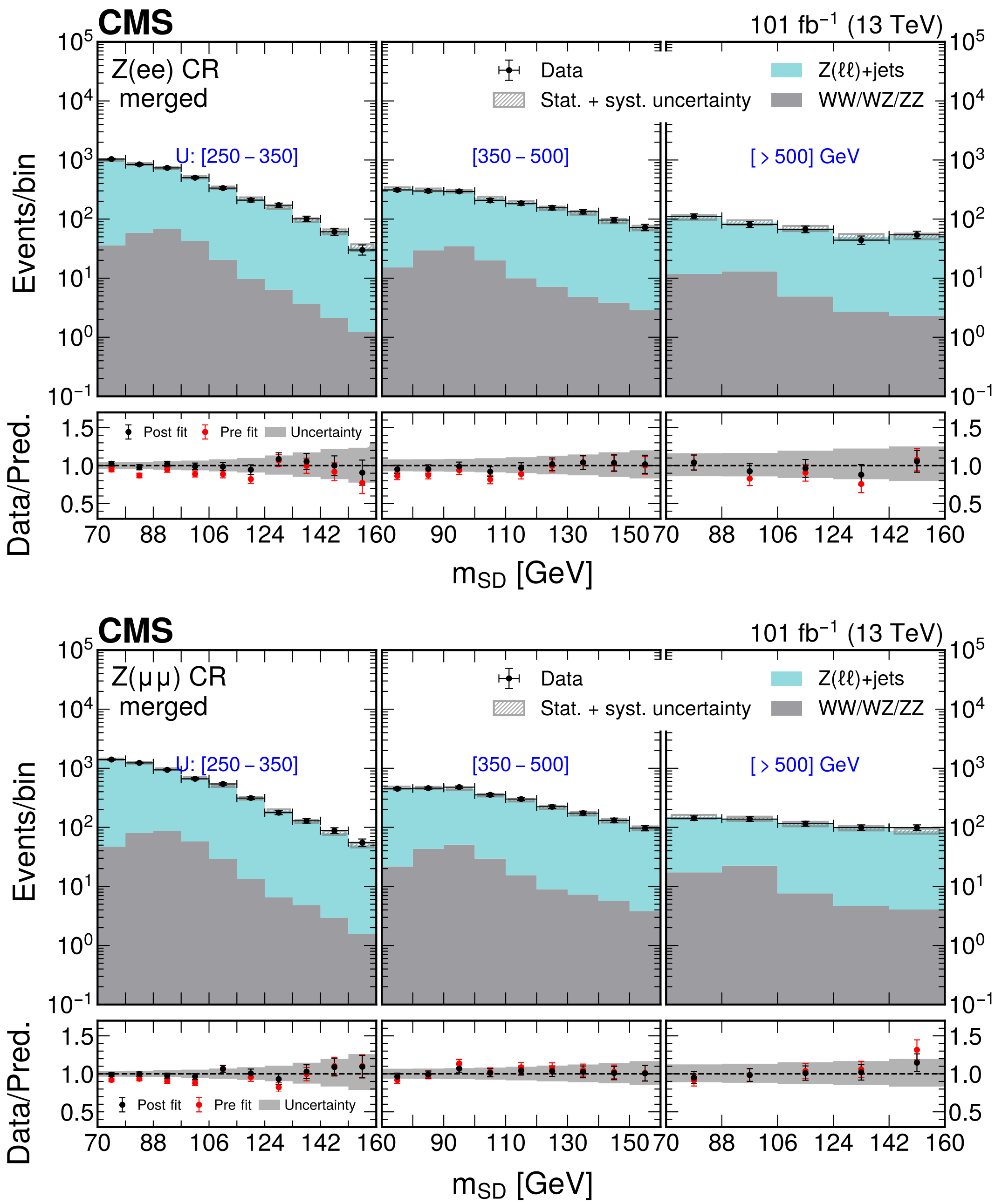

FIG. 5. The AK8 jet m_{SD} distributions after the simultaneous likelihood background-only fit sliced in three U bins, for the merged-category $Z(ee)$ (above) and $Z(\mu\mu)$ (below) CRs. The black markers with statistical uncertainty bars show the observed data, the stacked colored histograms show the predicted background, and the gray shading shows the systematic uncertainty in the prediction. The lower panels show the ratios of the observed data to the background predicted before (prefit in red) and after (postfit in black) the fit, with the gray bands indicating the postfit uncertainty obtained from combining all statistical and systematic sources.

For electrons, the systematic uncertainties associated with reconstruction (identification) have a normalization effect of 1–2 (1–5)%. An uncertainty of 6 (2)% is assigned to the tau lepton (photon) veto efficiency across all analysis regions.

The integrated luminosities for the 2016, 2017, and 2018 data-taking years have 1.2–2.5% individual uncertainties [66–69], while the overall uncertainty for the 2016–2018 period is 1.6%. A normalization uncertainty of 2.5% is applied to all background processes taken directly from the MC simulations.

Pileup modeling is addressed by reweighting the signal and background MC samples such that the number of true pileup interactions in simulation matches the pileup profile observed in data. The latter is determined using integrated luminosity per bunch crossing and assuming

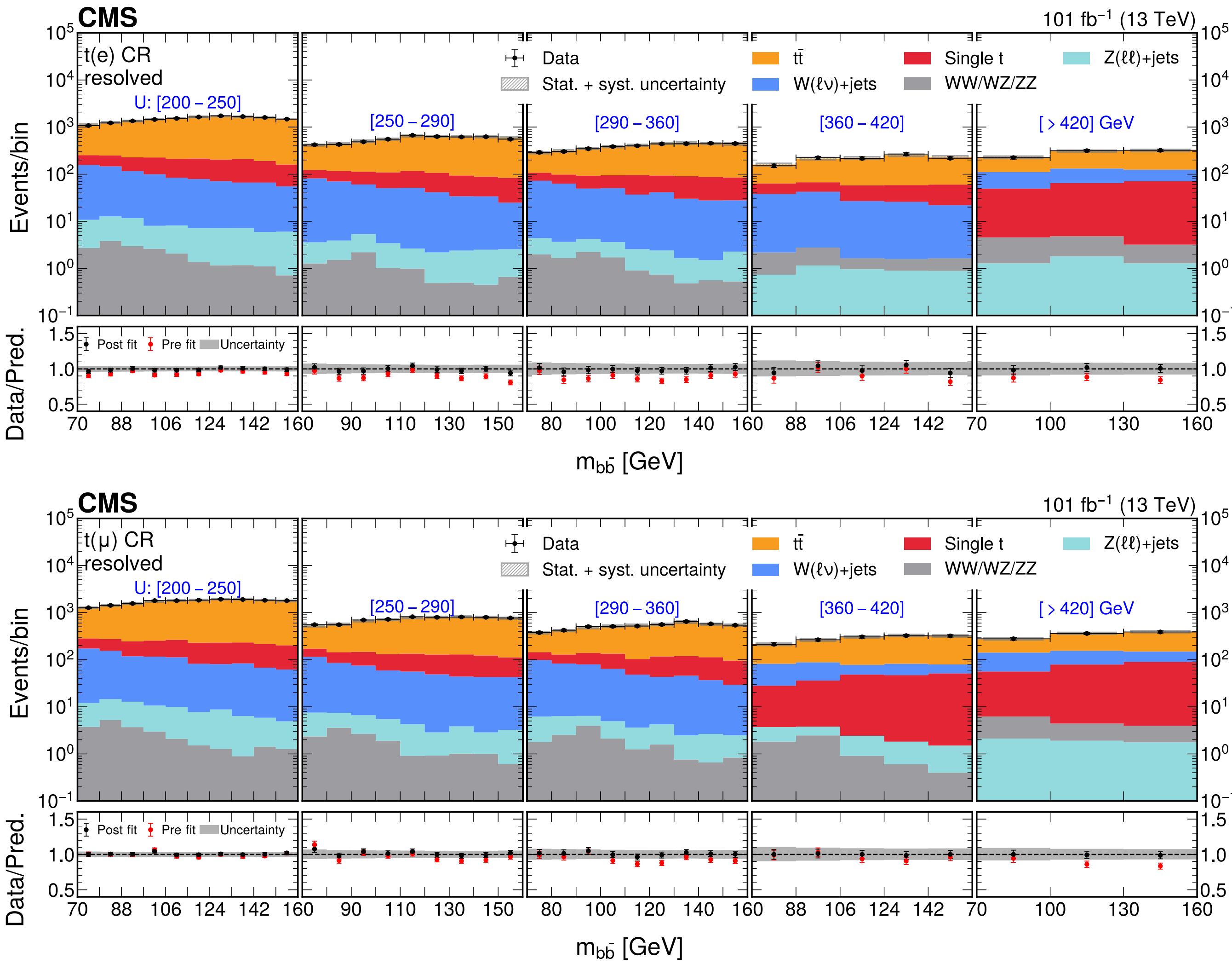

FIG. 6. The dijet $m_{b\bar{b}}$ distributions after the simultaneous likelihood background-only fit sliced in five U bins, for the resolved-category $t(e)$ (above) and $t(\mu)$ (below) CRs. The black markers with statistical uncertainty bars show the observed data, the stacked colored histograms show the predicted background, and the gray shading shows the systematic uncertainty in the prediction. The lower panels show the ratios of the observed data to the background predicted before (prefit in red) and after (postfit in black) the fit, with the gray bands indicating the postfit uncertainty obtained from combining all statistical and systematic sources.

the total inelastic cross section of 69.2 mb [70]. The systematic uncertainty from the pileup reweighting is evaluated by varying the total inelastic cross section by $\pm 4.6\%$.

During the 2017 data-taking period, a gradual shift in the timing of the inputs of the ECAL L1 trigger in the $|\eta| > 2.0$ region caused a trigger inefficiency, denoted as "prefiring" [25]. The trigger missed between 10 and 20% of the events containing an electron (of $p_{\mathrm{T}} \gtrsim 50$ GeV) or a jet (of $p_{\mathrm{T}} \gtrsim 100$ GeV) in the $2.5 < |\eta| < 3.0$ range, the exact loss depending on the p_{T} and η of the trigger object. Correction factors were computed from data and applied to the acceptance evaluated by simulation. The shape-based uncertainty for L1 prefiring has a normalization effect of 0.5–1%.

The JES corrections depend on jet p_{T} and η, and the uncertainties are split into 11 independent sources accounting for different experimental effects [52]. These systematic uncertainties are considered for all simulation-based processes, with a shape effect ranging from 0.1 to 5%. Differences in the JER between data and simulation are accounted for by smearing the p_{T} of jets in MC samples. The smearing factors and their uncertainties depend on the jet η. The shape-based uncertainty is assigned to all simulated processes, with an effect of around 4%. The change in the jet momentum due to JER smearing is propagated to the $p_{\mathrm{T}}^{\mathrm{miss}}$ computation.

The efficiency of the DeepJet [60,62] b tagging algorithm is parametrized as a function of jet p_{T}, η, and flavor, and is applied to AK4 b jets making the h candidate in the

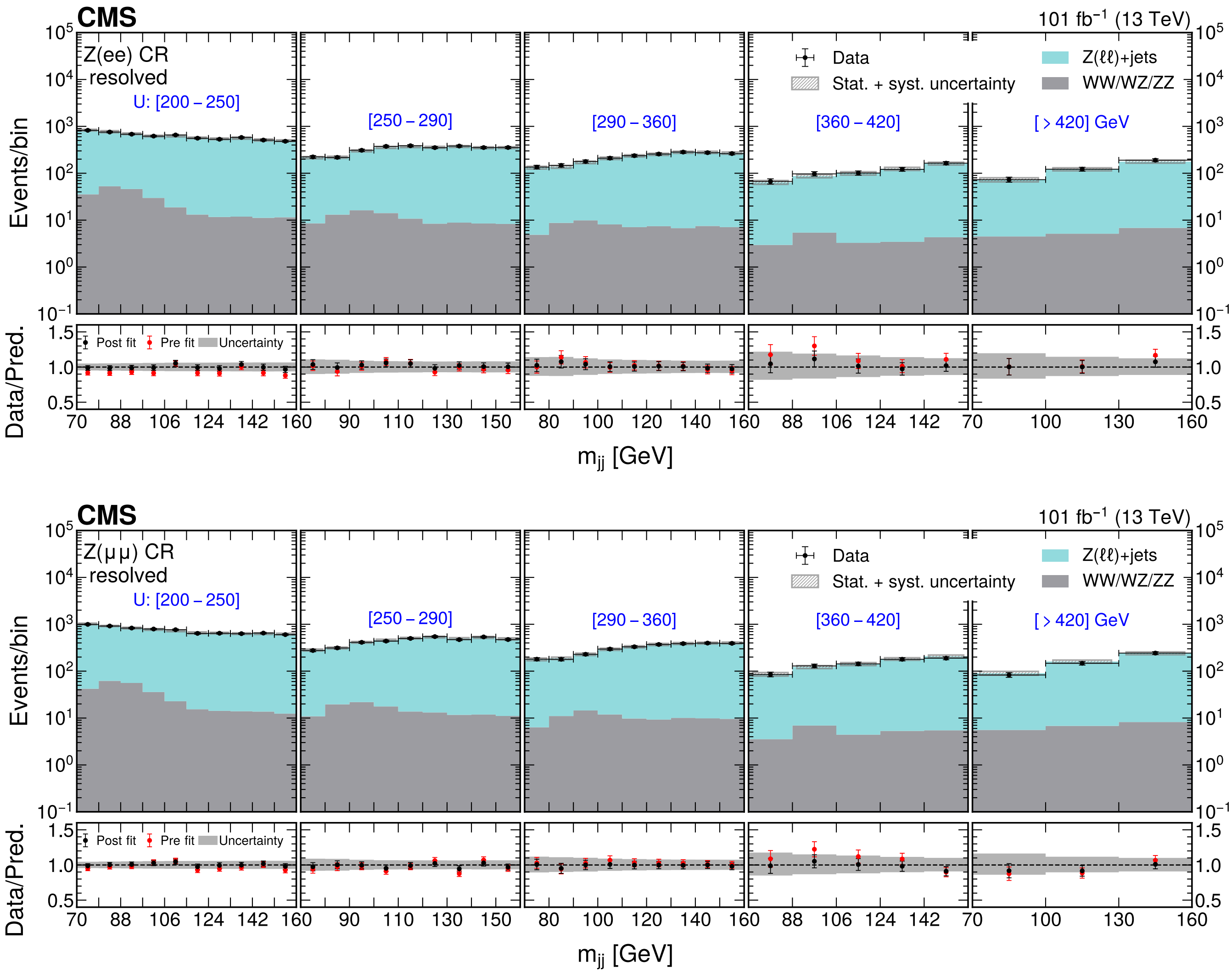

FIG. 7. The dijet m_{jj} distributions after the simultaneous likelihood background-only fit sliced in five U bins, for the resolved-category $Z(ee)$ (above) and $Z(\mu\mu)$ (below) CRs. The black markers with statistical uncertainty bars show the observed data, the stacked colored histograms show the predicted background, and the gray shading shows the systematic uncertainty in the prediction. The lower panels show the ratios of the observed data to the background predicted before (prefit in red) and after (postfit in black) the fit, with the gray bands indicating the postfit uncertainty obtained from combining all statistical and systematic sources.

resolved category. Discrepancies between data and simulation are corrected for using data-to-simulation correction factors. Shape-based uncertainties are computed separately for genuine b jets and misidentified b jets, with an average shape effect of 5%. For the merged category, an additional uncertainty in the ParticleNet-MD double-b tagging efficiency is applied to AK8 jets as a function of their p_T, with an average shape effect of around 2% [63,65].

Most experimental uncertainties are specific to each data set and are thus assumed to be uncorrelated between different data-taking periods. The uncertainties related to integrated luminosity, JES and JER, as well as those related to b tagging are partially correlated between the data-taking periods, which is implemented by splitting the total uncertainty into its correlated and uncorrelated components.

To mitigate discrepancies between the data and MC simulations in the p_T spectra of the top quarks in $t\bar{t}$ events, a parametric function is used to reweight the simulation. The uncertainty associated with this correction is estimated by comparing weighted and unweighted results, leading to a shape effect of around 7%. Shape uncertainties for the LO-to-NLO scale factors obtained for $W+$jets, $Z(\nu\nu)+$jets, and $Z(\ell\ell)+$jets processes [71] are considered to account for the missing higher-order corrections with QCD and EW terms. These shape uncertainties range from 5 to 20%, depending on the category, process, and boson p_T.

TABLE III. The sources of systematic uncertainty and the correlation scheme between the 2017 and 2018 data-taking periods, along with the type (normalization or shape) and their relative values.

Systematic source	Correlation between years	Type	Relative uncertainty [%]
b jet tagging efficiency	Partially correlated	Shape	1–5
b jet mistagging efficiency	Partially correlated	Shape	1–4
Double-b jet tagging efficiency	Uncorrelated	Shape	0–2
Jet energy scale	Partially correlated	Shape	0.1–5
Jet energy resolution	Uncorrelated	Shape	0–4
$p_{\mathrm{T}}^{\mathrm{miss}}$ trigger	Uncorrelated	Shape	1–2
Electron trigger	Uncorrelated	Shape	1–2
Electron reconstruction	Uncorrelated	Shape	1–2
Electron identification	Uncorrelated	Shape	1–5
Muon identification	Uncorrelated	Shape	<1
Muon isolation	Uncorrelated	Shape	<1
Integrated luminosity	Partially correlated	Normalization	1.2–2.5
Pileup reweighting	Uncorrelated	Shape	0–5
L1 prefiring	Uncorrelated	Shape	0.5–1
Tau lepton veto	Uncorrelated	Normalization	6
Photon veto	Uncorrelated	Normalization	2
Top quark p_{T} reweight	Correlated	Shape	0–7
$V+$jets p_{T} reweight	Correlated	Shape	5–20
PDF	Correlated	Shape	3–6
Renorm./fact. scale	Correlated	Shape	0–20
Cross section single top quark	Correlated	Normalization	10
Cross section $W+$jets	Correlated	Normalization	20
Cross section diboson	Correlated	Normalization	30
Cross section Higgs boson	Correlated	Normalization	5
Cross section signal	Correlated	Normalization	10

Uncertainties in the PDFs and those due to variations in the renormalization and factorization scales (μ_{R} and μ_{F}) impact both the shape and cross section of simulated processes. The PDF uncertainty is evaluated by reweighting simulated events using the set of PDF replicas from the NNPDF3.1 PDFs, following the PDF4LHC recommendations [72]. The envelope of variations is taken as the systematic uncertainty, with a typical effect of 3–6% depending on the process and category. Scale uncertainties are estimated by individually varying the μ_{R} and μ_{F} scales up and down by a factor of two, with the exception of simultaneously varying both up or down. The resulting uncertainty is 10–20%, and is treated as uncorrelated for the signal as well as the various background processes. These uncertainties are treated as correlated across categories and data-taking eras.

For background processes taken directly from the simulations, a normalization uncertainty of 10% is assigned to the single top quark process, 20% to the $W+$jets process, and 30% to the diboson process. These values are chosen based on existing experimental constraints [73–76]. For the signal process, a normalization uncertainty of 10% is assigned. A cross section uncertainty of 5% is assigned to the SM Higgs process. These uncertainties are correlated across categories and data-taking eras.

Table III summarizes the sources of systematic uncertainties considered in the analysis, the correlation scheme between the 2017 and 2018 data-taking periods, along with the type (normalization or shape) and the relative effect on the h candidate mass distribution sliced in $p_{\mathrm{T}}^{\mathrm{miss}}$ windows.

The MC bin-by-bin statistical uncertainties are handled using the CMS statistical tool Combine [77], which employs the "Barlow-Beeston-lite" technique [78]. A Poisson threshold of 10 events is set, such that for MC event counts exceeding 10, the uncertainty is modeled with a Gaussian distribution, while for counts below 10, a Poisson distribution is used to model per-process uncertainties in that bin.

The results based on the data set analyzed in this paper are further combined with the results from an earlier analysis based on data collected in 2016. The combination is performed by running a combined likelihood fit across all the analysis regions in all data sets. For this purpose, the uncertainty in integrated luminosity is partially correlated, and the PDF uncertainty is fully correlated between data-taking eras. The remaining uncertainty sources are treated as uncorrelated in the final combined fit.

VII. RESULTS

A maximum-likelihood fit [77] to extract the signal yield is performed to the SRs and CRs by combining the merged and resolved categories, as well as the 2017 and 2018 data sets. Figure 8 shows the h candidate mass distributions in

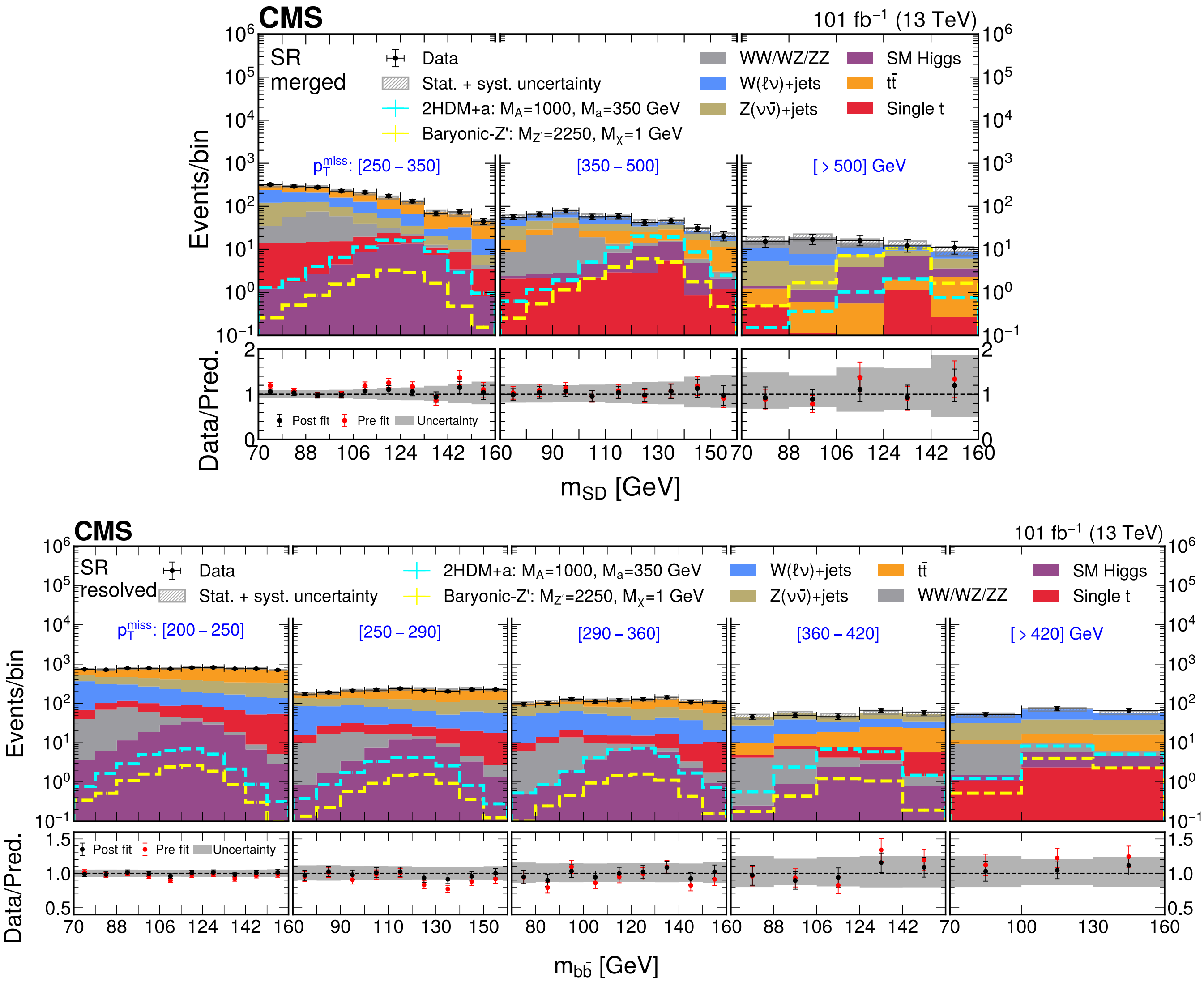

FIG. 8. The AK8 jet m_{SD} (above) and dijet $m_{b\bar{b}}$ (below) distributions after the simultaneous likelihood background-only fit sliced in three and five p_T^{miss} bins, for the merged- and resolved-category SRs, respectively. The black markers with statistical uncertainty bars show the observed data, the stacked colored histograms show the predicted background, and the gray shading shows the systematic uncertainty in the prediction. The signal predictions are overlaid as cyan and yellow dashed lines, one for each benchmark model. The lower panels show the ratios of the observed data to prefit (red points) and postfit (black points) background predictions, with the gray bands indicating the postfit uncertainty obtained from combining all statistical and systematic sources.

the m_{SD} and $m_{b\bar{b}}$ observables for the merged and resolved SRs, respectively, sliced into the three and five p_T^{miss} bins. The improved ratio of signal to background is evident as p_T^{miss} is increased, indicating the importance of fitting these regions separately, which increases signal sensitivity in the high p_T^{miss} regions while retaining the low p_T^{miss} regions that provide stronger constraints on the nuisance parameters describing the background. Superimposed on the data are the stacked histograms representing the background-only fit. The observed data show good agreement with this fit, and no significant excess of events is observed.

The results of this search are interpreted in two benchmark simplified models. An upper limit is computed on the cross section for the associated production of a dark matter candidate with a Higgs boson, calculated at 95% confidence level (CL) [77,79,80] using a modified frequentist approach [81] and asymptotic approximation [82].

In this method, background-only and signal-plus-background fits are performed for each signal model. The nuisance parameters are profiled in the signal fit, and the best-fit value of the signal strength modifier μ is extracted for each signal hypothesis. The expected limit is obtained from background-only pseudodata, while the observed limit is derived from the data. Deviations between the expected and observed limit can arise from statistical fluctuations and nuisance-parameter profiling even when

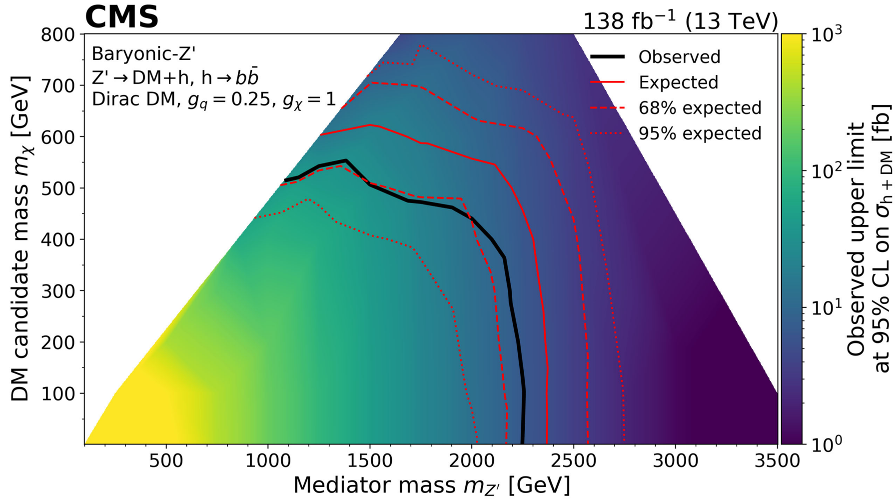

FIG. 9. Exclusion limits at 95% CL on the signal cross section $\sigma_{h+\mathrm{DM}}$ for the baryonic-Z' model as a function of $m_{Z'}$ and m_χ. The coupling parameters are fixed to $g_q = 0.25$ and $g_\chi = 1$. The areas within the solid black and red contours represent the exclusion regions where the theoretical cross sections are larger than the observed and expected experimental limits, respectively. The areas within the dashed and dotted red contours show the excluded regions at ± 1 and ± 2 standard deviations from the expected limits, respectively.

the background-only hypothesis provides the best fit to the observed data. A statistical combination is performed with the previous CMS analysis [19] that uses 2016 data. The interpretations presented in the following two sections are derived from the combined 2016–2018 data, with an integrated luminosity of 138 fb^{-1}. For the branching fraction of $h \to b\bar{b}$ we take 0.582 [83].

A. Baryonic-Z' model interpretation

The baryonic-Z' model provides a theoretical framework in which the DM candidate χ couples to SM quarks via a massive vector mediator, Z'. The dominant kinematic feature of this model is the presence of large $p_\mathrm{T}^\mathrm{miss}$ recoiling against a merged h candidate jet, which motivates the use of high-p_T h boson tagging. The parameter space is characterized primarily by the mediator and DM masses.

Figure 9 shows the exclusion limit at 95% CL on the signal cross section $\sigma_{h+\mathrm{DM}}$, as a two-dimensional scan over $m_{Z'}$ and m_χ. In this scan, the coupling between the mediator and SM quarks is fixed to $g_q = 0.25$, and the coupling between the mediator and DM particles is fixed to $g_\chi = 1$. For $m_\chi = 1$ GeV, values of $m_{Z'}$ below 2.25 TeV (2.35 TeV expected) are excluded. Masses of DM particles up to 550 GeV (600 GeV expected) are excluded for $m_{Z'} = 1.25$ TeV.

Compared to the previous result in Ref. [19] with the 2016 data set, the maximal exclusion limit in terms of $m_{Z'}$ is improved by 650 GeV (500 GeV expected) for $m_\chi = 1$ GeV. The higher luminosity data contributes around 300 GeV of expected improvement, with the additional 200 GeV of expected exclusion coming from the improved identification of boosted $h \to b\bar{b}$ decays with the latest tagging algorithms.

B. The 2HDM + a model interpretation

In the 2HDM + a model, the mono-Higgs signature arises from a scalar sector that includes a heavy pseudoscalar A and a light pseudoscalar mediator a, in addition to the h boson. When the mass hierarchy $m_A > m_a + m_h$ is satisfied, the process $A \to a + h$ becomes kinematically allowed, with the lighter pseudoscalar subsequently decaying invisibly to a pair of DM particles. The 2HDM + a framework offers a parameter space in which the production cross section and kinematic distributions are governed by model parameters such as the pseudoscalar masses m_A, m_a, the ratio of the vacuum expectation values $\tan\beta$, and the sine of the mixing angle, $\sin\theta$. The DM particle is assumed to have a mass of $m_\chi = 10$ GeV. The masses of the heavy scalar, heavy pseudoscalar, and the two charged scalars are fixed to the same value, i.e., $m_H = m_A = m_{H\pm}$ [17].

Figure 10 shows the observed and expected exclusion limits at 95% CL on the signal cross section $\sigma_{h+\mathrm{DM}}$ for four one-dimensional parameter scans (m_a, m_A, $\sin\theta$, and $\tan\beta$). For the m_a scan (upper left plot), the fixed parameters are $m_A = 1000$ GeV, $\sin\theta = 0.35$, and $\tan\beta = 1$. Light pseudoscalar masses below 360 GeV are excluded. For the m_A scan (upper right plot), the fixed parameters are $m_a = 350$ GeV, $\sin\theta = 0.35$, and $\tan\beta = 1$, with heavy pseudoscalar masses between 850 and 1300 GeV excluded. For the $\sin\theta$ scan (lower left plot), the fixed parameters are $m_a = 200$ GeV, $m_A = 600$ GeV, and $\tan\beta = 1$, with $\sin\theta$ values between 0.15 and 0.95 excluded. The variation of $\sin\theta$ leads to both rate and shape changes in the $p_\mathrm{T}^\mathrm{miss}$ spectrum, where the strong sensitivity is a result of the interplay of resonant and nonresonant contributions. The process $pp \to A \to ha \to h\chi\bar{\chi}$ scales as $\sin\theta\cos^2\theta$ and

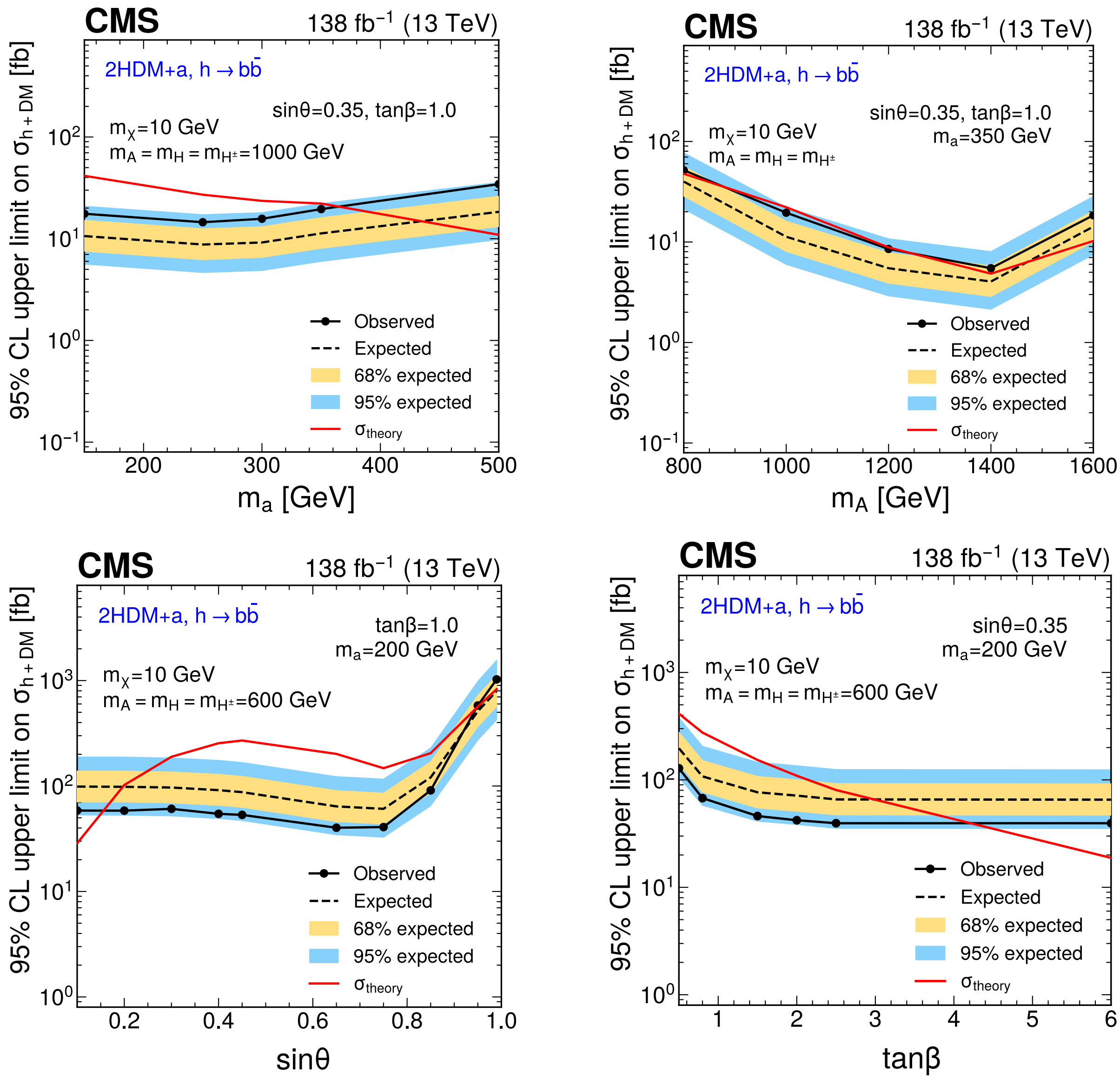

FIG. 10. Observed and expected exclusion limits at 95% CL on the signal cross section $\sigma_{h+\mathrm{DM}}$ for the 2HDM + a model as a function of the model parameters: m_a (upper left), m_A (upper right), $\sin\theta$ (lower left), and $\tan\beta$ (lower right) while fixing the values of the other parameters, as indicated in the legends. Different sets of model parameters are tested to probe distinct regions of phase space. Mass points below the solid red line are excluded.

the process $pp \to ha \to h\chi\bar{\chi}$ shows a $\sin\theta$ dependence, as detailed in Ref. [16]. Finally, for the $\tan\beta$ scan (lower right plot), the fixed parameters are $m_a = 200$ GeV, $m_A = 600$ GeV, and $\sin\theta = 0.35$, where $\tan\beta$ values below 4.2 are excluded by this analysis. As long as $m_\chi < m_a/2$, the decay is kinematically allowed, with very little dependence of either the rate or $p_\mathrm{T}^\mathrm{miss}$ spectrum on m_χ. We choose a benchmark value $m_\chi = 10$ GeV [16].

Motivated by Ref. [16], different sets of model parameters are tested, corresponding to $(m_A, m_a) = (1000, 350)$ GeV (Fig. 10 upper plots) and (600, 200) GeV (Fig. 10 lower plots). These choices probe distinct regions of phase space, resulting in signal events with different kinematic features. In particular, the former configuration yields higher $p_\mathrm{T}^\mathrm{miss}$, and together with different production cross sections, these variations result in differences between the observed and expected exclusion limits.

VIII. SUMMARY

A search for DM produced in association with a standard model Higgs boson decaying to a bottom quark-antiquark pair has been presented. The analysis is based on proton-proton collision data collected in 2017 and 2018 by the CMS experiment at $\sqrt{s} = 13$ TeV, corresponding to an integrated luminosity of 101 fb^{-1}. The search has been performed in merged and resolved categories to cover a wide range of Lorentz boosts of the Higgs boson. The signal is extracted using a simultaneous fit to the signal and control regions by combining the two categories. The observed data agree with the standard model background prediction, indicating no evidence for new physics. The results are statistically combined with an earlier search using 2016 data, corresponding to an integrated luminosity of 35.9 fb^{-1}.

The full 2016–2018 results have been interpreted in two simplified models, the baryonic-Z' model where a high mass resonance (Z') decays to a pair of DM particles and a Higgs boson, and the 2HDM $+\, a$ model where a heavy pseudoscalar couples to a Higgs boson and a lighter pseudoscalar that decays to a pair of DM particles. Exclusion limits are set on the model parameters at 95% confidence level. For the baryonic-Z' model, mediator Z' masses up to 2.25 TeV are excluded for a DM mass of 1 GeV, and DM particle masses up to 550 GeV are excluded for a 1.25 TeV Z' particle. In the 2HDM $+\, a$ framework, light pseudoscalar masses m_a below 360 GeV are excluded for a heavy pseudoscalar mass m_A of 1000 GeV, and m_A masses between 850 and 1300 GeV are excluded for m_a of 350 GeV. For the other model parameters, $\sin\theta$ values between 0.15 and 0.95 are excluded, while $\tan\beta$ values less than 4.2 are excluded. These results improve upon the previously existing CMS limits owing to the larger integrated luminosity and improved identification of $h \to b\bar{b}$ decay.

ACKNOWLEDGMENTS

We congratulate our colleagues in the CERN accelerator departments for the excellent performance of the LHC and thank the technical and administrative staffs at CERN and at other CMS institutes for their contributions to the success of the CMS effort. In addition, we gratefully acknowledge the computing centers and personnel of the Worldwide LHC Computing Grid and other centers for delivering so effectively the computing infrastructure essential to our analyses. Finally, we acknowledge the enduring support for the construction and operation of the LHC, the CMS detector, and the supporting computing infrastructure provided by the following funding agencies: SC (Armenia), BMBWF and FWF (Austria); FNRS and FWO (Belgium); CNPq, CAPES, FAPERJ, FAPERGS, and FAPESP (Brazil); MES and BNSF (Bulgaria); CERN; CAS, MoST, and NSFC (China); MINCIENCIAS (Colombia); MSES and CSF (Croatia); RIF (Cyprus); SENESCYT (Ecuador); ERC PRG, TARISTU24-TK10 and MoER TK202 (Estonia); Academy of Finland, MEC, and HIP (Finland); CEA and CNRS/IN2P3 (France); SRNSF (Georgia); BMFTR, DFG, and HGF (Germany); GSRI (Greece); NKFIH (Hungary); DAE and DST (India); IPM (Iran); SFI (Ireland); INFN (Italy); MSIT and NRF (Republic of Korea); MES (Latvia); LMTLT (Lithuania); MOE and UM (Malaysia); BUAP, CINVESTAV, CONACYT, LNS, SEP, and UASLP-FAI (Mexico); MOS (Montenegro); MBIE (New Zealand); PAEC (Pakistan); MES, NSC, and NAWA (Poland); FCT (Portugal); MESTD (Serbia); MICIU/AEI and PCTI (Spain); MOSTR (Sri Lanka); Swiss Funding Agencies (Switzerland); MST (Taipei); MHESI (Thailand); TUBITAK and TENMAK (Türkiye); NASU (Ukraine); STFC (United Kingdom); DOE and NSF (USA). Individuals have received support from the Marie-Curie program and the European Research Council and Horizon 2020 Grant, Contracts No. 675440, No. 724704, No. 752730, No. 758316, No. 765710, No. 824093, No. 101115353, No. 101002207, No. 101001205, and COST Action CA16108 (European Union); the Leventis Foundation; the Alfred P. Sloan Foundation; the Alexander von Humboldt Foundation; the Science Committee, Project No. 22rl-037 (Armenia); the Fonds pour la Formation *à la* Recherche dans l'Industrie et dans l'Agriculture (FRIA) and Fonds voor Wetenschappelijk Onderzoek Contract No. 1228724N (Belgium); the Beijing Municipal Science & Technology Commission, No. Z191100007219010, the Fundamental Research Funds for the Central Universities, the Ministry of Science and Technology of China under Grant No. 2023YFA1605804, the Natural Science Foundation of China under Grant No. 12535004, and USTC Research Funds of the Double First-Class Initiative No. YD2030002017 (China); the Ministry of Education, Youth and Sports (MEYS) of the Czech Republic; the Shota Rustaveli National Science Foundation, Grant No. FR-22-985 (Georgia); the Deutsche Forschungsgemeinschaft (DFG), among others, under Germany's Excellence Strategy—EXC 2121 "Quantum Universe"—390833306, and under Project No, 400140256—GRK2497; the Hellenic Foundation for Research and Innovation (HFRI), Project No. 2288 (Greece); the Hungarian Academy of Sciences, the New National Excellence Program—ÚNKP, the NKFIH research Grants No. K 131991, No. K 133046, No. K 138136, No. K 143460, No. K 143477, No. K 146913, No. K 146914, No. K 147048, No. 2020-2.2.1-ED-2021-00181, No. TKP2021-NKTA-64, and No. 2025-1.1.5-NEMZ_KI-2025-00004 (Hungary); the Council of Science and Industrial Research, India; ICSC—National Research Center for High Performance Computing, Big Data and Quantum Computing, FAIR—Future Artificial Intelligence Research, and CUP I53D23001070006 (Mission 4 Component 1), funded by the NextGenerationEU program (Italy); the Latvian Council of Science; the Ministry of Education and Science, Project No. 2022/WK/14, and the National Science Center, Contracts Opus 2021/41/B/ST2/01369, 2021/43/B/ST2/01552, 2023/49/B/ST2/03273, and the NAWA Contract No. BPN/PPO/2021/1/00011 (Poland); the Fundação para a Ciência e a Tecnologia, Grant No. CEECIND/01334/

2018 (Portugal); the National Priorities Research Program by Qatar National Research Fund; MICIU/AEI/10.13039/501100011033, ERDF/EU, "European Union NextGenerationEU/PRTR", and Programa Severo Ochoa del Principado de Asturias (Spain); the Chulalongkorn Academic into Its 2nd Century Project Advancement Project, the National Science, Research and Innovation Fund Program No. IND_FF_68_369_2300_097, and the Program Management Unit for Human Resources & Institutional Development, Research and Innovation, Grant No. B39G680009 (Thailand); the Kavli Foundation; the Nvidia Corporation; the SuperMicro Corporation; the Welch Foundation, Contract No. C-1845; and the Weston Havens Foundation (USA).

DATA AVAILABILITY

Release and preservation of data used by the CMS Collaboration as the basis for publications is guided by the CMS data preservation, reuse and open access policy [84].

[1] N. Aghanim *et al.* (Planck Collaboration), Planck 2018 results. I. Overview and the cosmological legacy of Planck, Astron. Astrophys. **641**, A1 (2020).

[2] J. L. Feng, Dark matter candidates from particle physics and methods of detection, Annu. Rev. Astron. Astrophys. **48**, 495 (2010).

[3] R. J. Scherrer and M. S. Turner, On the relic, cosmic abundance of stable weakly interacting massive particles, Phys. Rev. D **33**, 1585 (1986); **34**, 3263(E) (1986).

[4] G. Steigman and M. S. Turner, Cosmological constraints on the properties of weakly interacting massive particles, Nucl. Phys. B **253**, 375 (1985).

[5] G. Jungman, M. Kamionkowski, and K. Griest, Supersymmetric dark matter, Phys. Rep. **267**, 195 (1996).

[6] ATLAS Collaboration, Observation of a new particle in the search for the standard model Higgs boson with the ATLAS detector at the LHC, Phys. Lett. B **716**, 1 (2012).

[7] CMS Collaboration, Observation of a new boson at a mass of 125 GeV with the CMS experiment at the LHC, Phys. Lett. B **716**, 30 (2012).

[8] CMS Collaboration, Observation of a new boson with mass near 125 GeV in pp collisions at $\sqrt{s} = 7$ and 8 TeV, J. High Energy Phys. 06 (2013) 081.

[9] L. Carpenter, A. DiFranzo, M. Mulhearn, C. Shimmin, S. Tulin, and D. Whiteson, Mono-Higgs-boson: A new collider probe of dark matter, Phys. Rev. D **89**, 075017 (2014).

[10] A. Berlin, T. Lin, and L.-T. Wang, Mono-Higgs detection of dark matter at the LHC, J. High Energy Phys. 06 (2014) 078.

[11] A. A. Petrov and W. Shepherd, Searching for dark matter at LHC with mono-Higgs production, Phys. Lett. B **730**, 178 (2014).

[12] G. Bertone, D. Hooper, and J. Silk, Particle dark matter: Evidence, candidates and constraints, Phys. Rep. **405**, 279 (2005).

[13] C. P. Burgess, M. Pospelov, and T. ter Veldhuis, The minimal model of nonbaryonic dark matter: A singlet scalar, Nucl. Phys. **B619**, 709 (2001).

[14] J. March-Russell, S. M. West, D. Cumberbatch, and D. Hooper, Heavy dark matter through the Higgs portal, J. High Energy Phys. 07 (2008) 058.

[15] D. Abercrombie *et al.*, Dark matter benchmark models for early LHC Run 2 searches: Report of the ATLAS/CMS dark matter forum, Phys. Dark Universe **27**, 100371 (2020).

[16] T. Abe *et al.*, LHC Dark Matter Working Group: Next-generation spin-0 dark matter models, Phys. Dark Universe **27**, 100351 (2020).

[17] M. Bauer, U. Haisch, and F. Kahlhoefer, Simplified dark matter models with two Higgs doublets: I. Pseudoscalar mediators, J. High Energy Phys. 05 (2017) 138.

[18] G. C. Branco, P. M. Ferreira, L. Lavoura, M. N. Rebelo, M. Sher, and J. P. Silva, Theory and phenomenology of two-Higgs-doublet models, Phys. Rep. **516**, 1 (2012).

[19] CMS Collaboration, Search for dark matter produced in association with a Higgs boson decaying to a pair of bottom quarks in proton-proton collisions at $\sqrt{s} = 13$ TeV, Eur. Phys. J. C **79**, 280 (2019).

[20] ATLAS Collaboration, Search for dark matter produced in association with a standard model Higgs boson decaying into b-quarks using the full Run 2 dataset from the ATLAS detector, J. High Energy Phys. 11 (2021) 209.

[21] J. Thaler and K. Van Tilburg, Identifying boosted objects with N-subjettiness, J. High Energy Phys. 03 (2011) 015.

[22] HEPData record for this analysis (2026), 10.17182/hepdata.167738.

[23] CMS Collaboration, The CMS experiment at the CERN LHC, J. Instrum. **3**, S08004 (2008).

[24] CMS Collaboration, Development of the CMS detector for the CERN LHC Run 3, J. Instrum. **19**, P05064 (2023).

[25] CMS Collaboration, Performance of the CMS Level-1 trigger in proton-proton collisions at $\sqrt{s} = 13$ TeV, J. Instrum. **15**, P10017 (2020).

[26] CMS Collaboration, The CMS trigger system, J. Instrum. **12**, P01020 (2016).

[27] R. D. Ball, V. Bertone, S. Carrazza, L. Del Debbio, S. Forte, P. Groth-Merrild, A. Guffanti, N. P. Hartland, Z. Kassabov, J. I. Latorre, E. R. Nocera, J. Rojo, L. Rottoli, E. Slade, and M. Ubiali (NNPDF Collaboration), Parton distributions from high-precision collider data, Eur. Phys. J. C **77**, 663 (2017).

[28] CMS Collaboration, Event generator tunes obtained from underlying event and multiparton scattering measurements, Eur. Phys. J. C **76**, 155 (2016).

[29] T. Sjöstrand, S. Ask, J. R. Christiansen, R. Corke, N. Desai, P. Ilten, S. Mrenna, S. Prestel, C. O. Rasmussen, and P. Z. Skands, An introduction to PYTHIA8.2, Comput. Phys. Commun. **191**, 159 (2015).
[30] CMS Collaboration, Extraction and validation of a new set of CMS PYTHIA8 tunes from underlying-event measurements, Eur. Phys. J. C **80**, 4 (2020).
[31] S. Agostinelli *et al.* (GEANT4 Collaboration), Geant4—a simulation toolkit, Nucl. Instrum. Methods Phys. Res., Sect. A **506**, 250 (2003).
[32] J. Alwall, R. Frederix, S. Frixione, V. Hirschi, F. Maltoni, O. Mattelaer, H.-S. Shao, T. Stelzer, P. Torrielli, and M. Zaro, The automated computation of tree-level and next-to-leading order differential cross sections, and their matching to parton shower simulations, J. High Energy Phys. 07 (2014) 079.
[33] P. Nason, A new method for combining NLO QCD with shower Monte Carlo algorithms, J. High Energy Phys. 11 (2004) 040.
[34] S. Frixione, P. Nason, and C. Oleari, Matching NLO QCD computations with parton shower simulations: The POWHEG method, J. High Energy Phys. 11 (2007) 070.
[35] S. Alioli, P. Nason, C. Oleari, and E. Re, A general framework for implementing NLO calculations in shower Monte Carlo programs: The POWHEG BOX, J. High Energy Phys. 06 (2010) 043.
[36] CMS Collaboration, Measurement of differential cross sections for the production of top quark pairs and of additional jets in lepton + jets events from pp collisions at $\sqrt{s} = 13$ TeV, Phys. Rev. D **97**, 112003 (2018).
[37] R. Frederix, E. Re, and P. Torrielli, Single-top t-channel hadroproduction in the four-flavors scheme with POWHEG and aMC@NLO, J. High Energy Phys. 09 (2012) 130.
[38] E. Re, Single-top Wt-channel production matched with parton showers using the POWHEG method, Eur. Phys. J. C **71**, 1547 (2011).
[39] J. Alwall, S. Höche, F. Krauss, N. Lavesson, L. Lönnblad, F. Maltoni, M. L. Mangano, M. Moretti, C. G. Papadopoulos, F. Piccinini, S. Schumann, M. Treccani, J. Winter, and M. Worek, Comparative study of various algorithms for the merging of parton showers and matrix elements in hadronic collisions, Eur. Phys. J. C **53**, 473 (2008).
[40] R. Frederix and S. Frixione, Merging meets matching in MC@NLO, J. High Energy Phys. 12 (2012) 061.
[41] CMS Collaboration, Particle-flow reconstruction and global event description with the CMS detector, J. Instrum. **12**, P10003 (2017).
[42] CMS Collaboration, Technical proposal for the Phase-II upgrade of the Compact Muon Solenoid, CMS Technical Proposal CERN-LHCC-2015-010, CMS-TDR-15-02, 2015.
[43] CMS Collaboration, Electron and photon reconstruction and identification with the CMS experiment at the CERN LHC, J. Instrum. **16**, P05014 (2020).
[44] CMS Collaboration, ECAL 2016 refined calibration and Run 2 summary plots, CMS Detector Performance Note CMS-DP-2020-021, 2020.
[45] CMS Collaboration, Performance of the CMS muon detector and muon reconstruction with proton-proton collisions at $\sqrt{s} = 13$ TeV, J. Instrum. **13**, P06015 (2018).
[46] CMS Collaboration, Performance of reconstruction and identification of τ leptons decaying to hadrons and ν_τ in pp collisions at $\sqrt{s} = 13$ TeV, J. Instrum. **13**, P10005 (2018).
[47] CMS Collaboration, Identification of hadronic tau lepton decays using a deep neural network, J. Instrum. **17**, P07023 (2022).
[48] M. Cacciari, G. P. Salam, and G. Soyez, The anti-k_T jet clustering algorithm, J. High Energy Phys. 04 (2008) 063.
[49] M. Cacciari, G. P. Salam, and G. Soyez, FastJet user manual, Eur. Phys. J. C **72**, 1896 (2012).
[50] CMS Collaboration, Pileup mitigation at CMS in 13 TeV data, J. Instrum. **15**, P09018 (2020).
[51] D. Bertolini, P. Harris, M. Low, and N. Tran, Pileup per particle identification, J. High Energy Phys. 10 (2014) 059.
[52] CMS Collaboration, Jet energy scale and resolution in the CMS experiment in pp collisions at 8 TeV, J. Instrum. **12**, P02014 (2016).
[53] CMS Collaboration, Jet energy scale and resolution measurements with legacy Run 2 data collected by CMS at 13 TeV, CMS Detector Performance Note CMS-DP-2021-033, 2021.
[54] CMS Collaboration, Performance of missing transverse momentum reconstruction in proton-proton collisions at $\sqrt{s} = 13$ TeV using the CMS detector, J. Instrum. **14**, P07004 (2019).
[55] Y. L. Dokshitzer, G. D. Leder, S. Moretti, and B. R. Webber, Better jet clustering algorithms, J. High Energy Phys. 08 (1997) 001.
[56] M. Wobisch and T. Wengler, Hadronization corrections to jet cross-sections in deep inelastic scattering, in *Proceedings of the Workshop on Monte Carlo Generators for HERA Physics: Hamburg, Germany, 1998* (DESY, Hamburg, Germany, 1998), p. 270; arXiv:hep-ph/9907280.
[57] M. Dasgupta, A. Fregoso, S. Marzani, and G. P. Salam, Towards an understanding of jet substructure, J. High Energy Phys. 09 (2013) 029.
[58] J. M. Butterworth, A. R. Davison, M. Rubin, and G. P. Salam, Jet substructure as a new Higgs search channel at the LHC, Phys. Rev. Lett. **100**, 242001 (2008).
[59] A. J. Larkoski, S. Marzani, G. Soyez, and J. Thaler, Soft drop, J. High Energy Phys. 05 (2014) 146.
[60] E. Bols, J. Kieseler, M. Verzetti, M. Stoye, and A. Stakia, Jet flavour classification using DeepJet, J. Instrum. **15**, P12012 (2020).
[61] CMS Collaboration, Identification of heavy-flavour jets with the CMS detector in pp collisions at 13 TeV, J. Instrum. **13**, P05011 (2018).
[62] CMS Collaboration, Performance summary of AK4 jet b tagging with data from proton-proton collisions at 13 TeV with the CMS detector, CMS Detector Performance Note CMS-DP-2023-005, 2023.
[63] H. Qu and L. Gouskos, Jet tagging via particle clouds, Phys. Rev. D **101**, 056019 (2020).
[64] CMS Collaboration, Calibration of the mass-decorrelated ParticleNet tagger for boosted $b\bar{b}$ and $c\bar{c}$ jets using LHC Run 2 data, CMS Detector Performance Note CMS-DP-2022-005, 2024.
[65] CMS Collaboration, Performance of heavy-flavour jet identification in Lorentz-boosted topologies in proton-proton collisions at $\sqrt{s} = 13$ TeV, J. Instrum. **20**, P11006 (2025).

[66] CMS Collaboration, Precision luminosity measurement in proton-proton collisions at $\sqrt{s} = 13$ TeV in 2015 and 2016 at CMS, Eur. Phys. J. C **81**, 800 (2021).
[67] CMS Collaboration, CMS luminosity measurement for the 2017 data-taking period at $\sqrt{s} = 13$ TeV, CMS Physics Analysis Summary CMS-PAS-LUM-17-004, 2018, https://cds.cern.ch/record/2621960.
[68] CMS Collaboration, CMS luminosity measurement for the 2018 data-taking period at $\sqrt{s} = 13$ TeV, CMS Physics Analysis Summary CMS-PAS-LUM-18-002, 2019, https://cds.cern.ch/record/2676164.
[69] CMS Collaboration, Precision luminosity measurement in proton-proton collisions at $\sqrt{s} = 13$ TeV with the CMS detector, CMS Physics Analysis Summary CMS-PAS-LUM-20-001, 2025, https://cds.cern.ch/record/2940794.
[70] CMS Collaboration, Measurement of the inelastic proton-proton cross section at $\sqrt{s} = 13$ TeV, J. High Energy Phys. 07 (2018) 161.
[71] CMS Collaboration, Search for new particles in events with energetic jets and large missing transverse momentum in proton-proton collisions at $\sqrt{s} = 13$ TeV, J. High Energy Phys. 11 (2021) 153.
[72] J. Butterworth *et al.*, PDF4LHC recommendations for LHC Run 2, J. Phys. G **43**, 023001 (2016).
[73] CMS Collaboration, Observation of the associated production of a single top quark and a W boson in pp collisions at $\sqrt{s} = 8$ TeV, Phys. Rev. Lett. **112**, 231802 (2014).
[74] CMS Collaboration, Measurements of inclusive W and Z cross sections in pp collisions at $\sqrt{s} = 7$ TeV, J. High Energy Phys. 01 (2011) 080.
[75] CMS Collaboration, Measurement of the ZZ production cross section and $Z \to \ell^+\ell^-\ell'^+\ell'^-$ branching fraction in pp collisions at $\sqrt{s} = 13$ TeV, Phys. Lett. B **763**, 280 (2016).
[76] CMS Collaboration, Measurement of the inclusive and differential WZ production cross sections, polarization angles, and triple gauge couplings in pp collisions at $\sqrt{s} = 13$ TeV, J. High Energy Phys. 07 (2022) 032.
[77] CMS Collaboration, The CMS statistical analysis and combination tool: Combine, Comput. Software Big Sci. **8**, 19 (2024).
[78] R. Barlow and C. Beeston, Fitting using finite Monte Carlo samples, Comput. Phys. Commun. **77**, 219 (1993).
[79] T. Junk, Confidence level computation for combining searches with small statistics, Nucl. Instrum. Methods Phys. Res., Sect. A **434**, 435 (1999).
[80] A. L. Read, Presentation of search results: The CL_s technique, J. Phys. G **28**, 2693 (2002).
[81] ATLAS and CMS Collaborations, and LHC Higgs Combination Group, Procedure for the LHC Higgs boson search combination in Summer 2011, Technical Report, CMS-NOTE-2011-005, ATL-PHYS-PUB-2011-11, CERN, Geneva, Switzerland, 2011, https://cds.cern.ch/record/1379837.
[82] G. Cowan, K. Cranmer, E. Gross, and O. Vitells, Asymptotic formulae for likelihood-based tests of new physics, Eur. Phys. J. C **71**, 1554 (2011); **73**, 2501(E) (2013).
[83] S. Navas *et al.* (Particle Data Group), Review of particle physics, Phys. Rev. D **110**, 030001 (2024).
[84] CMS Collaboration, 2020 CMS data preservation, re-use and open access policy. CERN Open Data Portal (2020), 10.7483/OPENDATA.CMS.1BNU.8V1W.

A. Hayrapetyan,[1] V. Makarenko,[1] A. Tumasyan,[1,b] W. Adam,[2] L. Benato,[2] T. Bergauer,[2] M. Dragicevic,[2] C. Giordano,[2] P. S. Hussain,[2] M. Jeitler,[2,c] N. Krammer,[2] A. Li,[2] D. Liko,[2] M. Matthewman,[2] J. Schieck,[2,c] R. Schöfbeck,[2,c] D. Schwarz,[2] M. Shooshtari,[2] M. Sonawane,[2] W. Waltenberger,[2] C.-E. Wulz,[2,c] T. Janssen,[3] H. Kwon,[3] D. Ocampo Henao,[3] T. Van Laer,[3] P. Van Mechelen,[3] J. Bierkens,[4] N. Breugelmans,[4] J. D'Hondt,[4] S. Dansana,[4] A. De Moor,[4] M. Delcourt,[4] F. Heyen,[4] Y. Hong,[4] P. Kashko,[4] S. Lowette,[4] I. Makarenko,[4] D. Müller,[4] J. Song,[4] S. Tavernier,[4] M. Tytgat,[4,d] G. P. Van Onsem,[4] S. Van Putte,[4] D. Vannerom,[4] B. Bilin,[5] B. Clerbaux,[5] A. K. Das,[5] I. De Bruyn,[5] G. De Lentdecker,[5] H. Evard,[5] L. Favart,[5] P. Gianneios,[5] A. Khalilzadeh,[5] F. A. Khan,[5] A. Malara,[5] M. A. Shahzad,[5] A. Sharma,[5] L. Thomas,[5] M. Vanden Bemden,[5] C. Vander Velde,[5] P. Vanlaer,[5] F. Zhang,[5] M. De Coen,[6] D. Dobur,[6] G. Gokbulut,[6] D. Marckx,[6] K. Skovpen,[6] A. M. Tomaru,[6] N. Van Den Bossche,[6] J. van der Linden,[6] J. Vandenbroeck,[6] L. Wezenbeek,[6] H. Aarup Petersen,[7] S. Bein,[7] A. Benecke,[7] A. Bethani,[7] G. Bruno,[7] A. Cappati,[7] J. De Favereau De Jeneret,[7] C. Delaere,[7] F. Gameiro Casalinho,[7] A. Giammanco,[7] A. O. Guzel,[7] V. Lemaitre,[7] J. Lidrych,[7] P. Malek,[7] P. Mastrapasqua,[7] S. Turkcapar,[7] G. A. Alves,[8] M. Barroso Ferreira Filho,[8] E. Coelho,[8] C. Hensel,[8] D. Matos Figueiredo,[8] T. Menezes De Oliveira,[8] C. Mora Herrera,[8] P. Rebello Teles,[8] M. Soeiro,[8] E. J. Tonelli Manganote,[8,e] A. Vilela Pereira,[8] W. L. Aldá Júnior,[9] H. Brandao Malbouisson,[9] W. Carvalho,[9] J. Chinellato,[9,f] M. Costa Reis,[9] E. M. Da Costa,[9] G. G. Da Silveira,[9,g] D. De Jesus Damiao,[9] S. Fonseca De Souza,[9] R. Gomes De Souza,[9] S. S. Jesus,[9] T. Laux Kuhn,[9,g] M. Macedo,[9] K. Mota Amarilo,[9] L. Mundim,[9] H. Nogima,[9] J. P. Pinheiro,[9] A. Santoro,[9] A. Sznajder,[9] M. Thiel,[9] F. Torres Da Silva De Araujo,[9,h] C. A. Bernardes,[10,g] L. Calligaris,[10] F. Damas,[10] T. R. Fernandez Perez Tomei,[10] E. M. Gregores,[10] B. Lopes Da Costa,[10] I. Maietto Silverio,[10] P. G. Mercadante,[10] S. F. Novaes,[10] B. Orzari,[10] Sandra S. Padula,[10] V. Scheurer,[10] A. Aleksandrov,[11]

G. Antchev,[11] P. Danev,[11] R. Hadjiiska,[11] P. Iaydjiev,[11] M. Shopova,[11] G. Sultanov,[11] A. Dimitrov,[12] L. Litov,[12] B. Pavlov,[12] P. Petkov,[12] A. Petrov,[12] S. Keshri,[13] D. Laroze,[13] S. Thakur,[13] W. Brooks,[14] T. Cheng,[15] T. Javaid,[15] L. Wang,[15] L. Yuan,[15] Z. Hu,[16] Z. Liang,[16] J. Liu,[16] X. Wang,[16] H. Yang,[16] G. M. Chen,[17,i] H. S. Chen,[17,i] M. Chen,[17,i] Y. Chen,[17] Q. Hou,[17] X. Hou,[17] F. Iemmi,[17] C. H. Jiang,[17] H. Liao,[17] G. Liu,[17] Z.-A. Liu,[17,j] J. N. Song,[17,j] S. Song,[17] J. Tao,[17] C. Wang,[17,i] J. Wang,[17] H. Zhang,[17] J. Zhao,[17] A. Agapitos,[18] Y. Ban,[18] A. Carvalho Antunes De Oliveira,[18] S. Deng,[18] B. Guo,[18] Q. Guo,[18] C. Jiang,[18] A. Levin,[18] C. Li,[18] Q. Li,[18] Y. Mao,[18] S. Qian,[18] S. J. Qian,[18] X. Qin,[18] C. Quaranta,[18] X. Sun,[18] D. Wang,[18] J. Wang,[18] M. Zhang,[18] Y. Zhao,[18] C. Zhou,[18] S. Yang,[19] Z. You,[20] K. Jaffel,[21] N. Lu,[21] G. Bauer,[22,k,l] Z. Cui,[22,l] B. Li,[22,m] H. Wang,[22] K. Yi,[22,n] J. Zhang,[22] Y. Li,[23] Y. Zhou,[23,o] Z. Lin,[24] C. Lu,[24] M. Xiao,[24,p] C. Avila,[25] D. A. Barbosa Trujillo,[25] A. Cabrera,[25] C. Florez,[25] J. Fraga,[25] J. A. Reyes Vega,[25] C. Rendón,[26] M. Rodriguez,[26] A. A. Ruales Barbosa,[26] J. D. Ruiz Alvarez,[26] N. Godinovic,[27] D. Lelas,[27] A. Sculac,[27] M. Kovac,[28] A. Petkovic,[28] T. Sculac,[28] P. Bargassa,[29] V. Brigljevic,[29] B. K. Chitroda,[29] D. Ferencek,[29] K. Jakovcic,[29] A. Starodumov,[29] T. Susa,[29] A. Attikis,[30] K. Christoforou,[30] S. Konstantinou,[30] C. Leonidou,[30] L. Paizanos,[30] F. Ptochos,[30] P. A. Razis,[30] H. Rykaczewski,[30] H. Saka,[30] A. Stepennov,[30] M. Finger,[31,a] M. Finger Jr.,[31] E. Ayala,[32] E. Carrera Jarrin,[33] S. Elgammal,[34,q] A. Ellithi Kamel,[34,r] A. Hussein,[35] H. Mohammed,[35] M. Kadastik,[36] T. Lange,[36] C. Nielsen,[36] J. Pata,[36] M. Raidal,[36] N. Seeba,[36] L. Tani,[36] E. Brücken,[37] A. Milieva,[37] K. Osterberg,[37] M. Voutilainen,[37] F. Garcia,[38] P. Inkaew,[38] K. T. S. Kallonen,[38] R. Kumar Verma,[38] T. Lampén,[38] K. Lassila-Perini,[38] B. Lehtela,[38] S. Lehti,[38] T. Lindén,[38] N. R. Mancilla Xinto,[38] M. Myllymäki,[38] M. m. Rantanen,[38] S. Saariokari,[38] N. T. Toikka,[38] J. Tuominiemi,[38] N. Bin Norjoharuddeen,[39] H. Kirschenmann,[39] P. Luukka,[39] H. Petrow,[39] M. Besancon,[40] F. Couderc,[40] M. Dejardin,[40] D. Denegri,[40] P. Devouge,[40] J. L. Faure,[40] F. Ferri,[40] P. Gaigne,[40] S. Ganjour,[40] P. Gras,[40] G. Hamel de Monchenault,[40] M. Kumar,[40] V. Lohezic,[40] Y. Maidannyk,[40] J. Malcles,[40] F. Orlandi,[40] L. Portales,[40] S. Ronchi,[40] M. Ö. Sahin,[40] A. Savoy-Navarro,[40,s] P. Simkina,[40] M. Titov,[40] M. Tornago,[40] R. Amella Ranz,[41] F. Beaudette,[41] G. Boldrini,[41] P. Busson,[41] C. Charlot,[41] M. Chiusi,[41] T. D. Cuisset,[41] O. Davignon,[41] A. De Wit,[41] T. Debnath,[41] I. T. Ehle,[41] S. Ghosh,[41] A. Gilbert,[41] R. Granier de Cassagnac,[41] L. Kalipoliti,[41] M. Manoni,[41] M. Nguyen,[41] S. Obraztsov,[41] C. Ochando,[41] R. Salerno,[41] J. B. Sauvan,[41] Y. Sirois,[41] G. Sokmen,[41] L. Urda Gómez,[41] A. Zabi,[41] A. Zghiche,[41] J.-L. Agram,[42,t] J. Andrea,[42] D. Bloch,[42] J.-M. Brom,[42] E. C. Chabert,[42] C. Collard,[42] G. Coulon,[42] S. Falke,[42] U. Goerlach,[42] R. Haeberle,[42] A.-C. Le Bihan,[42] M. Meena,[42] O. Poncet,[42] G. Saha,[42] P. Vaucelle,[42] A. Di Florio,[43] D. Amram,[44] S. Beauceron,[44] B. Blancon,[44] G. Boudoul,[44] N. Chanon,[44] D. Contardo,[44] P. Depasse,[44] H. El Mamouni,[44] J. Fay,[44] S. Gascon,[44] M. Gouzevitch,[44] C. Greenberg,[44] G. Grenier,[44] B. Ille,[44] E. Jourd'Huy,[44] M. Lethuillier,[44] B. Massoteau,[44] L. Mirabito,[44] A. Purohit,[44] M. Vander Donckt,[44] J. Xiao,[44] G. Adamov,[45] I. Lomidze,[45] Z. Tsamalaidze,[45,u] V. Botta,[46] S. Consuegra Rodríguez,[46] L. Feld,[46] K. Klein,[46] M. Lipinski,[46] P. Nattland,[46] V. Oppenländer,[46] A. Pauls,[46] D. Pérez Adán,[46] N. Röwert,[46] C. Daumann,[47] S. Diekmann,[47] N. Eich,[47] D. Eliseev,[47] F. Engelke,[47] J. Erdmann,[47] M. Erdmann,[47] B. Fischer,[47] T. Hebbeker,[47] K. Hoepfner,[47] F. Ivone,[47] A. Jung,[47] N. Kumar,[47] M. y. Lee,[47] F. Mausolf,[47] M. Merschmeyer,[47] A. Meyer,[47] A. Pozdnyakov,[47] W. Redjeb,[47] H. Reithler,[47] U. Sarkar,[47] V. Sarkisovi,[47] A. Schmidt,[47] C. Seth,[47] A. Sharma,[47] J. L. Spah,[47] V. Vaulin,[47] S. Zaleski,[47] M. R. Beckers,[48] C. Dziwok,[48] G. Flügge,[48] N. Hoeflich,[48] T. Kress,[48] A. Nowack,[48] O. Pooth,[48] A. Stahl,[48] A. Zotz,[48] A. Abel,[49] M. Aldaya Martin,[49] J. Alimena,[49] S. Amoroso,[49] Y. An,[49] I. Andreev,[49] J. Bach,[49] S. Baxter,[49] M. Bayatmakou,[49] H. Becerril Gonzalez,[49] O. Behnke,[49] A. Belvedere,[49] F. Blekman,[49,v] K. Borras,[49,w] A. Campbell,[49] S. Chatterjee,[49] L. X. Coll Saravia,[49] G. Eckerlin,[49] D. Eckstein,[49] E. Gallo,[49,v] A. Geiser,[49] V. Guglielmi,[49] M. Guthoff,[49] A. Hinzmann,[49] L. Jeppe,[49] M. Kasemann,[49] C. Kleinwort,[49] R. Kogler,[49] M. Komm,[49] D. Krücker,[49] W. Lange,[49] D. Leyva Pernia,[49] K.-Y. Lin,[49] K. Lipka,[49,x] W. Lohmann,[49,y] J. Malvaso,[49] R. Mankel,[49] I.-A. Melzer-Pellmann,[49] M. Mendizabal Morentin,[49] A. B. Meyer,[49] G. Milella,[49] K. Moral Figueroa,[49] A. Mussgiller,[49] L. P. Nair,[49] J. Niedziela,[49] A. Nürnberg,[49] J. Park,[49] E. Ranken,[49] A. Raspereza,[49] D. Rastorguev,[49] L. Rygaard,[49] M. Scham,[49,z,w] S. Schnake,[49,w] P. Schütze,[49] C. Schwanenberger,[49,v] D. Selivanova,[49] K. Sharko,[49] M. Shchedrolosiev,[49] D. Stafford,[49] M. Torkian,[49] A. Ventura Barroso,[49] R. Walsh,[49] D. Wang,[49] Q. Wang,[49] K. Wichmann,[49] L. Wiens,[49,w] C. Wissing,[49] Y. Yang,[49] S. Zakharov,[49] A. Zimermmane Castro Santos,[49] A. R. Alves Andrade,[50] M. Antonello,[50] S. Bollweg,[50]

M. Bonanomi,[50] K. El Morabit,[50] Y. Fischer,[50] M. Frahm,[50] E. Garutti,[50] A. Grohsjean,[50] A. A. Guvenli,[50] J. Haller,[50] D. Hundhausen,[50] G. Kasieczka,[50] P. Keicher,[50] R. Klanner,[50] W. Korcari,[50] T. Kramer,[50] C. c. Kuo,[50] F. Labe,[50] J. Lange,[50] A. Lobanov,[50] L. Moureaux,[50] K. Nikolopoulos,[50] A. Paasch,[50] K. J. Pena Rodriguez,[50] N. Prouvost,[50] B. Raciti,[50] M. Rieger,[50] D. Savoiu,[50] P. Schleper,[50] M. Schröder,[50] J. Schwandt,[50] M. Sommerhalder,[50] H. Stadie,[50] G. Steinbrück,[50] R. Ward,[50] B. Wiederspan,[50] M. Wolf,[50] C. Yede,[50] S. Brommer,[51] A. Brusamolino,[51] E. Butz,[51] Y. M. Chen,[51] T. Chwalek,[51] A. Dierlamm,[51] G. G. Dincer,[51] D. Druzhkin,[51] U. Elicabuk,[51] N. Faltermann,[51] M. Giffels,[51] A. Gottmann,[51] F. Hartmann,[51,aa] M. Horzela,[51] F. Hummer,[51] U. Husemann,[51] J. Kieseler,[51] M. Klute,[51] J. Knolle,[51] R. Kunnilan Muhammed Rafeek,[51] O. Lavoryk,[51] J. M. Lawhorn,[51] A. Lintuluoto,[51] S. Maier,[51] A. A. Monsch,[51] M. Mormile,[51] Th. Müller,[51] E. Pfeffer,[51] M. Presilla,[51] G. Quast,[51] K. Rabbertz,[51] B. Regnery,[51] R. Schmieder,[51] N. Shadskiy,[51] I. Shvetsov,[51] H. J. Simonis,[51] L. Sowa,[51] L. Stockmeier,[51] K. Tauqeer,[51] M. Toms,[51] B. Topko,[51] N. Trevisani,[51] C. Verstege,[51] T. Voigtländer,[51] R. F. Von Cube,[51] J. Von Den Driesch,[51] M. Wassmer,[51] C. Winter,[51] R. Wolf,[51] W. D. Zeuner,[51] X. Zuo,[51] G. Anagnostou,[52] G. Daskalakis,[52] A. Kyriakis,[52] G. Melachroinos,[53] Z. Painesis,[53] I. Paraskevas,[53] N. Saoulidou,[53] K. Theofilatos,[53] E. Tziaferi,[53] E. Tzovara,[53] K. Vellidis,[53] I. Zisopoulos,[53] T. Chatzistavrou,[54] G. Karapostoli,[54] K. Kousouris,[54] E. Siamarkou,[54] G. Tsipolitis,[54] I. Bestintzanos,[55] I. Evangelou,[55] C. Foudas,[55] P. Katsoulis,[55] P. Kokkas,[55] P. G. Kosmoglou Kioseoglou,[55] N. Manthos,[55] I. Papadopoulos,[55] J. Strologas,[55] C. Hajdu,[56] D. Horvath,[56,bb,cc] K. Márton,[56] A. J. Rádl,[56,dd] F. Sikler,[56] V. Veszpremi,[56] M. Csanád,[57] K. Farkas,[57] A. Fehérkuti,[57,ee] M. M. A. Gadallah,[57,ff] Á. Kadlecsik,[57] M. León Coello,[57] G. Pásztor,[57] G. I. Veres,[57] B. Ujvari,[58] G. Zilizi,[58] G. Bencze,[59] S. Czellar,[59] J. Molnar,[59] Z. Szillasi,[59] T. Csorgo,[60,ee] F. Nemes,[60,ee] T. Novak,[60] I. Szanyi,[60,gg] S. Bahinipati,[61] S. Nayak,[61] R. Raturi,[61] S. Bansal,[62] S. B. Beri,[62] V. Bhatnagar,[62] S. Chauhan,[62] N. Dhingra,[62,hh] A. Kaur,[62] H. Kaur,[62] M. Kaur,[62] S. Kumar,[62] T. Sheokand,[62] J. B. Singh,[62] A. Singla,[62] A. Bhardwaj,[63] A. Chhetri,[63] B. C. Choudhary,[63] A. Kumar,[63] A. Kumar,[63] M. Naimuddin,[63] S. Phor,[63] K. Ranjan,[63] M. K. Saini,[63] P. Palni,[64] S. Acharya,[65,ii] B. Gomber,[65] S. Mukherjee,[66] S. Bhattacharya,[67] S. Das Gupta,[67] S. Dutta,[67] S. Dutta,[67] S. Sarkar,[67] M. M. Ameen,[68] P. K. Behera,[68] S. Chatterjee,[68] G. Dash,[68] A. Dattamunsi,[68] P. Jana,[68] P. Kalbhor,[68] S. Kamble,[68] J. R. Komaragiri,[68,jj] T. Mishra,[68] P. R. Pujahari,[68] A. K. Sikdar,[68] R. K. Singh,[68] P. Verma,[68] S. Verma,[68] A. Vijay,[68] B. K. Sirasva,[69] L. Bhatt,[70] S. Dugad,[70] G. B. Mohanty,[70] M. Shelake,[70] P. Suryadevara,[70] A. Bala,[71] S. Banerjee,[71] S. Barman,[71,kk] R. M. Chatterjee,[71] M. Guchait,[71] Sh. Jain,[71] A. Jaiswal,[71] S. Kumar,[71] M. Maity,[71,kk] G. Majumder,[71] K. Mazumdar,[71] S. Parolia,[71] R. Saxena,[71] A. Thachayath,[71] D. Maity,[72,ll] P. Mal,[72] K. Naskar,[72,ll] A. Nayak,[72,ll] K. Pal,[72] P. Sadangi,[72] S. K. Swain,[72] S. Varghese,[72,ll] D. Vats,[72,ll] S. Dube,[73] P. Hazarika,[73] B. Kansal,[73] A. Laha,[73] R. Sharma,[73] S. Sharma,[73] K. Y. Vaish,[73] S. Ghosh,[74] H. Bakhshiansohi,[75,mm] A. Jafari,[75,nn] V. Sedighzadeh Dalavi,[75] M. Zeinali,[75,oo] S. Bashiri,[76] S. Chenarani,[76,pp] S. M. Etesami,[76] Y. Hosseini,[76] M. Khakzad,[76] E. Khazaie,[76] M. Mohammadi Najafabadi,[76] S. Tizchang,[76,qq] M. Felcini,[77] M. Grunewald,[77] M. Abbrescia,[78a,78b] M. Barbieri,[78a,78b] M. Buonsante,[78a,78b] A. Colaleo,[78a,78b] D. Creanza,[78a,78c] N. De Filippis,[78a,78c] M. De Palma,[78a,78b] W. Elmetenawee,[78a,78b,rr] N. Ferrara,[78a,78c] L. Fiore,[78a] L. Generoso,[78a,78b] L. Longo,[78a] M. Louka,[78a,78b] G. Maggi,[78a,78c] M. Maggi,[78a] I. Margjeka,[78a] V. Mastrapasqua,[78a,78b] S. My,[78a,78b] F. Nenna,[78a,78b] S. Nuzzo,[78a,78b] A. Pellecchia,[78a,78b] A. Pompili,[78a,78b] G. Pugliese,[78a,78c] R. Radogna,[78a,78b] D. Ramos,[78a] A. Ranieri,[78a] L. Silvestris,[78a] F. M. Simone,[78a,78c] Ü. Sözbilir,[78a] A. Stamerra,[78a,78b] D. Troiano,[78a,78b] R. Venditti,[78a,78b] P. Verwilligen,[78a] A. Zaza,[78a,78b] G. Abbiendi,[79a] C. Battilana,[79a,79b] D. Bonacorsi,[79a,79b] P. Capiluppi,[79a,79b] F. R. Cavallo,[79a] M. Cuffiani,[79a,79b] T. Diotalevi,[79a,79b] F. Fabbri,[79a] A. Fanfani,[79a,79b] R. Farinelli,[79a] D. Fasanella,[79a] P. Giacomelli,[79a] L. Guiducci,[79a,79b] S. Lo Meo,[79a,ss] M. Lorusso,[79a,79b] L. Lunerti,[79a] S. Marcellini,[79a] G. Masetti,[79a] F. L. Navarria,[79a,79b] G. Paggi,[79a,79b] A. Perrotta,[79a] A. M. Rossi,[79a,79b] S. Rossi Tisbeni,[79a,79b] T. Rovelli,[79a,79b] G. P. Siroli,[79a,79b] S. Costa,[80a,80b,tt] A. Di Mattia,[80a] A. Lapertosa,[80a] R. Potenza,[80a,80b] A. Tricomi,[80a,80b,tt] J. Altork,[81a,81b] P. Assiouras,[81a] G. Barbagli,[81a] G. Bardelli,[81a] M. Bartolini,[81a,81b] A. Calandri,[81a,81b] B. Camaiani,[81a,81b] A. Cassese,[81a] R. Ceccarelli,[81a] V. Ciulli,[81a,81b] C. Civinini,[81a] R. D'Alessandro,[81a,81b] L. Damenti,[81a,81b] E. Focardi,[81a,81b] T. Kello,[81a] G. Latino,[81a,81b] P. Lenzi,[81a,81b] M. Lizzo,[81a] M. Meschini,[81a] S. Paoletti,[81a] A. Papanastassiou,[81a,81b] G. Sguazzoni,[81a] L. Viliani,[81a] L. Benussi,[82] S. Bianco,[82] S. Meola,[82,uu] D. Piccolo,[82] M. Alves Gallo Pereira,[83a] F. Ferro,[83a] E. Robutti,[83a] S. Tosi,[83a,83b] A. Benaglia,[84a] F. Brivio,[84a]

V. Camagni,[84a,84b] F. Cetorelli,[84a,84b] F. De Guio,[84a,84b] M. E. Dinardo,[84a,84b] P. Dini,[84a] S. Gennai,[84a]
R. Gerosa,[84a,84b] A. Ghezzi,[84a,84b] P. Govoni,[84a,84b] L. Guzzi,[84a] M. R. Kim,[84a] G. Lavizzari,[84a,84b]
M. T. Lucchini,[84a,84b] M. Malberti,[84a] S. Malvezzi,[84a] A. Massironi,[84a] D. Menasce,[84a] L. Moroni,[84a]
M. Paganoni,[84a,84b] S. Palluotto,[84a,84b] D. Pedrini,[84a] A. Perego,[84a,84b] G. Pizzati,[84a,84b] T. Tabarelli de Fatis,[84a,84b]
S. Buontempo,[85a] C. Di Fraia,[85a,85b] F. Fabozzi,[85a,85c] L. Favilla,[85a,85d] A. O. M. Iorio,[85a,85b] L. Lista,[85a,85b,vv]
P. Paolucci,[85a,aa] B. Rossi,[85a] P. Azzi,[86a] N. Bacchetta,[86a,ww] M. Bellato,[86a] D. Bisello,[86a,86b] P. Bortignon,[86a,86c]
G. Bortolato,[86a,86b] A. C. M. Bulla,[86a,86c] P. Checchia,[86a] T. Dorigo,[86a,xx] F. Gasparini,[86a,86b] U. Gasparini,[86a,86b]
S. Giorgetti,[86a] E. Lusiani,[86a] M. Margoni,[86a,86b] A. T. Meneguzzo,[86a,86b] J. Pazzini,[86a,86b] F. Primavera,[86a,86b]
P. Ronchese,[86a,86b] R. Rossin,[86a,86b] F. Simonetto,[86a,86b] M. Tosi,[86a,86b] A. Triossi,[86a,86b] S. Ventura,[86a]
M. Zanetti,[86a,86b] P. Zotto,[86a,86b] A. Zucchetta,[86a,86b] A. Braghieri,[87a] S. Calzaferri,[87a,87b] P. Montagna,[87a,87b]
M. Pelliccioni,[87a,87b] V. Re,[87a] C. Riccardi,[87a,87b] P. Salvini,[87a] I. Vai,[87a,87b] P. Vitulo,[87a,87b] S. Ajmal,[88a,88b]
M. E. Ascioti,[88a,88b] G. M. Bilei,[88a,a] C. Carrivale,[88a,88b] D. Ciangottini,[88a,88b] L. Della Penna,[88a,88b] L. Fanò,[88a,88b]
V. Mariani,[88a,88b] M. Menichelli,[88a] F. Moscatelli,[88a,yy] A. Rossi,[88a,88b] A. Santocchia,[88a,88b] D. Spiga,[88a]
T. Tedeschi,[88a,88b] C. Aimè,[89a,89b] C. A. Alexe,[89a,89c] P. Asenov,[89a,89b] P. Azzurri,[89a] G. Bagliesi,[89a]
L. Bianchini,[89a,89b] T. Boccali,[89a] E. Bossini,[89a] D. Bruschini,[89a,89c] R. Castaldi,[89a] F. Cattafesta,[89a,89c]
M. A. Ciocci,[89a,89d] M. Cipriani,[89a,89b] R. Dell'Orso,[89a] S. Donato,[89a,89b] R. Forti,[89a,89b] A. Giassi,[89a]
F. Ligabue,[89a,89c] A. C. Marini,[89a,89b] A. Messineo,[89a,89b] S. Mishra,[89a] V. K. Muraleedharan Nair Bindhu,[89a,89b]
S. Nandan,[89a] F. Palla,[89a] M. Riggirello,[89a,89c] A. Rizzi,[89a,89b] G. Rolandi,[89a,89c] S. Roy Chowdhury,[89a,zz]
T. Sarkar,[89a] A. Scribano,[89a] P. Solanki,[89a,89b] P. Spagnolo,[89a] F. Tenchini,[89a,89b] R. Tenchini,[89a] G. Tonelli,[89a,89b]
N. Turini,[89a,89d] F. Vaselli,[89a,89c] A. Venturi,[89a] P. G. Verdini,[89a] P. Akrap,[90a,90b] C. Basile,[90a,90b] S. C. Behera,[90a]
F. Cavallari,[90a] L. Cunqueiro Mendez,[90a,90b] F. De Riggi,[90a,90b] D. Del Re,[90a,90b] E. Di Marco,[90a] M. Diemoz,[90a]
F. Errico,[90a] L. Frosina,[90a,90b] R. Gargiulo,[90a,90b] B. Harikrishnan,[90a,90b] F. Lombardi,[90a,90b] E. Longo,[90a,90b]
L. Martikainen,[90a,90b] J. Mijuskovic,[90a,90b] G. Organtini,[90a,90b] N. Palmeri,[90a,90b] R. Paramatti,[90a,90b]
S. Rahatlou,[90a,90b] C. Rovelli,[90a] F. Santanastasio,[90a,90b] L. Soffi,[90a] V. Vladimirov,[90a,90b] N. Amapane,[91a,91b]
R. Arcidiacono,[91a,91c] S. Argiro,[91a,91b] M. Arneodo,[91a,91c,a] N. Bartosik,[91a,91c] R. Bellan,[91a,91b] A. Bellora,[91a,91b]
C. Biino,[91a] C. Borca,[91a,91b] N. Cartiglia,[91a] M. Costa,[91a,91b] R. Covarelli,[91a,91b] N. Demaria,[91a] L. Finco,[91a]
M. Grippo,[91a,91b] B. Kiani,[91a,91b] L. Lanteri,[91a,91b] F. Legger,[91a] F. Luongo,[91a,91b] C. Mariotti,[91a] S. Maselli,[91a]
A. Mecca,[91a,91b] L. Menzio,[91a,91b] P. Meridiani,[91a] E. Migliore,[91a,91b] M. Monteno,[91a] M. M. Obertino,[91a,91b]
G. Ortona,[91a] L. Pacher,[91a,91b] N. Pastrone,[91a] M. Ruspa,[91a,91c] F. Siviero,[91a,91b] V. Sola,[91a,91b] A. Solano,[91a,91b]
A. Staiano,[91a] C. Tarricone,[91a,91b] D. Trocino,[91a] G. Umoret,[91a,91b] E. Vlasov,[91a,91b] R. White,[91a,91b]
J. Babbar,[92a,92b] S. Belforte,[92a] V. Candelise,[92a,92b] M. Casarsa,[92a] F. Cossutti,[92a] K. De Leo,[92a]
G. Della Ricca,[92a,92b] R. Delli Gatti,[92a,92b] S. Dogra,[93] J. Hong,[93] J. Kim,[93] T. Kim,[93] D. Lee,[93] H. Lee,[93] J. Lee,[93]
S. W. Lee,[93] C. S. Moon,[93] Y. D. Oh,[93] S. Sekmen,[93] B. Tae,[93] Y. C. Yang,[93] M. S. Kim,[94] G. Bak,[95]
P. Gwak,[95] H. Kim,[95] D. H. Moon,[95] J. Seo,[95] E. Asilar,[96] F. Carnevali,[96] J. Choi,[96,aaa] T. J. Kim,[96]
Y. Ryou,[96] S. Ha,[97] S. Han,[97] B. Hong,[97] J. Kim,[97] K. Lee,[97] K. S. Lee,[97] S. Lee,[97] J. Yoo,[97] J. Goh,[98]
J. Shin,[98] S. Yang,[98] Y. Kang,[99] H. S. Kim,[99] Y. Kim,[99] B. Ko,[99] S. Lee,[99] J. Almond,[100] J. H. Bhyun,[100]
J. Choi,[100] J. Choi,[100] W. Jun,[100] H. Kim,[100] J. Kim,[100] T. Kim,[100] Y. Kim,[100] Y. W. Kim,[100] S. Ko,[100] H. Lee,[100]
J. Lee,[100] J. Lee,[100] B. H. Oh,[100] J. Shin,[100] U. K. Yang,[100] I. Yoon,[100] W. Jang,[101] D. Y. Kang,[101] D. Kim,[101]
S. Kim,[101] J. S. H. Lee,[101] Y. Lee,[101] I. C. Park,[101] Y. Roh,[101] I. J. Watson,[101] G. Cho,[102] K. Hwang,[102]
B. Kim,[102] S. Kim,[102] K. Lee,[102] H. D. Yoo,[102] Y. Lee,[103] I. Yu,[103] T. Beyrouthy,[104] Y. Gharbia,[104]
F. Alazemi,[105] K. Dreimanis,[106] O. M. Eberlins,[106] A. Gaile,[106] C. Munoz Diaz,[106] D. Osite,[106] G. Pikurs,[106]
R. Plese,[106] A. Potrebko,[106] M. Seidel,[106] D. Sidiropoulos Kontos,[106] N. R. Strautnieks,[107] M. Ambrozas,[108]
A. Juodagalvis,[108] S. Nargelas,[108] A. Rinkevicius,[108] G. Tamulaitis,[108] I. Yusuff,[109,bbb] Z. Zolkapli,[109]
J. F. Benitez,[110] A. Castaneda Hernandez,[110] A. Cota Rodriguez,[110] L. E. Cuevas Picos,[110] H. A. Encinas Acosta,[110]
L. G. Gallegos Maríñez,[110] J. A. Murillo Quijada,[110] L. Valencia Palomo,[110] G. Ayala,[111] H. Castilla-Valdez,[111]
H. Crotte Ledesma,[111] R. Lopez-Fernandez,[111] J. Mejia Guisao,[111] R. Reyes-Almanza,[111]
A. Sánchez Hernández,[111] C. Oropeza Barrera,[112] D. L. Ramirez Guadarrama,[112] M. Ramírez García,[112]
I. Bautista,[113] F. E. Neri Huerta,[113] I. Pedraza,[113] H. A. Salazar Ibarguen,[113] C. Uribe Estrada,[113] I. Bubanja,[114]
N. Raicevic,[114] P. H. Butler,[115] A. Ahmad,[116] M. I. Asghar,[116] A. Awais,[116] M. I. M. Awan,[116] W. A. Khan,[116]

V. Avati,[117] L. Forthomme,[117] L. Grzanka,[117] M. Malawski,[117] K. Piotrzkowski,[117] M. Bluj,[118] M. Górski,[118] M. Kazana,[118] M. Szleper,[118] P. Zalewski,[118] K. Bunkowski,[119] K. Doroba,[119] A. Kalinowski,[119] M. Konecki,[119] J. Krolikowski,[119] A. Muhammad,[119] P. Fokow,[120] K. Pozniak,[120] W. Zabolotny,[120] M. Araujo,[121] D. Bastos,[121] C. Beirão Da Cruz E Silva,[121] A. Boletti,[121] M. Bozzo,[121] T. Camporesi,[121] G. Da Molin,[121] M. Gallinaro,[121] J. Hollar,[121] N. Leonardo,[121] G. B. Marozzo,[121] A. Petrilli,[121] M. Pisano,[121] J. Seixas,[121] J. Varela,[121] J. W. Wulff,[121] P. Adzic,[122] L. Markovic,[122] P. Milenovic,[122] V. Milosevic,[122] D. Devetak,[123] M. Dordevic,[123] J. Milosevic,[123] L. Nadderd,[123] V. Rekovic,[123] M. Stojanovic,[123] M. Alcalde Martinez,[124] J. Alcaraz Maestre,[124] Cristina F. Bedoya,[124] J. A. Brochero Cifuentes,[124] Oliver M. Carretero,[124] M. Cepeda,[124] M. Cerrada,[124] N. Colino,[124] B. De La Cruz,[124] A. Delgado Peris,[124] A. Escalante Del Valle,[124] D. Fernández Del Val,[124] J. P. Fernández Ramos,[124] J. Flix,[124] M. C. Fouz,[124] M. Gonzalez Hernandez,[124] O. Gonzalez Lopez,[124] S. Goy Lopez,[124] J. M. Hernandez,[124] M. I. Josa,[124] J. Llorente Merino,[124] C. Martin Perez,[124] E. Martin Viscasillas,[124] D. Moran,[124] C. M. Morcillo Perez,[124] Á. Navarro Tobar,[124] R. Paz Herrera,[124] A. Pérez-Calero Yzquierdo,[124] J. Puerta Pelayo,[124] I. Redondo,[124] J. Vazquez Escobar,[124] J. F. de Trocóniz,[125] B. Alvarez Gonzalez,[126] J. Ayllon Torresano,[126] A. Cardini,[126] J. Cuevas,[126] J. Del Riego Badas,[126] D. Estrada Acevedo,[126] J. Fernandez Menendez,[126] S. Folgueras,[126] I. Gonzalez Caballero,[126] P. Leguina,[126] M. Obeso Menendez,[126] E. Palencia Cortezon,[126] J. Prado Pico,[126] A. Soto Rodríguez,[126] P. Vischia,[126] S. Blanco Fernández,[127] I. J. Cabrillo,[127] A. Calderon,[127] J. Duarte Campderros,[127] M. Fernandez,[127] G. Gomez,[127] C. Lasaosa García,[127] R. Lopez Ruiz,[127] C. Martinez Rivero,[127] P. Martinez Ruiz del Arbol,[127] F. Matorras,[127] P. Matorras Cuevas,[127] E. Navarrete Ramos,[127] J. Piedra Gomez,[127] C. Quintana San Emeterio,[127] L. Scodellaro,[127] I. Vila,[127] R. Vilar Cortabitarte,[127] J. M. Vizan Garcia,[127] B. Kailasapathy,[128,ccc] D. D. C. Wickramarathna,[128] W. G. D. Dharmaratna,[129,ddd] K. Liyanage,[129] N. Perera,[129] D. Abbaneo,[130] C. Amendola,[130] R. Ardino,[130] E. Auffray,[130] J. Baechler,[130] D. Barney,[130] J. Bendavid,[130] M. Bianco,[130] A. Bocci,[130] L. Borgonovi,[130] C. Botta,[130] A. Bragagnolo,[130] C. E. Brown,[130] C. Caillol,[130] G. Cerminara,[130] P. Connor,[130] K. Cormier,[130] D. d'Enterria,[130] A. Dabrowski,[130] A. David,[130] A. De Roeck,[130] M. M. Defranchis,[130] M. Deile,[130] M. Dobson,[130] P. J. Fernández Manteca,[130] B. A. Fontana Santos Alves,[130] E. Fontanesi,[130] W. Funk,[130] A. Gaddi,[130] S. Giani,[130] D. Gigi,[130] K. Gill,[130] F. Glege,[130] M. Glowacki,[130] A. Gruber,[130] J. Hegeman,[130] J. K. Heikkilä,[130] R. Hofsaess,[130] B. Huber,[130] T. James,[130] P. Janot,[130] O. Kaluzinska,[130] O. Karacheban,[130,y] G. Karathanasis,[130] S. Laurila,[130] P. Lecoq,[130] E. Leutgeb,[130] C. Lourenço,[130] A.-M. Lyon,[130] M. Magherini,[130] L. Malgeri,[130] M. Mannelli,[130] A. Mehta,[130] F. Meijers,[130] J. A. Merlin,[130] S. Mersi,[130] E. Meschi,[130] M. Migliorini,[130] F. Monti,[130] F. Moortgat,[130] M. Mulders,[130] M. Musich,[130] I. Neutelings,[130] S. Orfanelli,[130] F. Pantaleo,[130] M. Pari,[130] G. Petrucciani,[130] A. Pfeiffer,[130] M. Pierini,[130] M. Pitt,[130] H. Qu,[130] D. Rabady,[130] A. Reimers,[130] B. Ribeiro Lopes,[130] F. Riti,[130] P. Rosado,[130] M. Rovere,[130] H. Sakulin,[130] R. Salvatico,[130] S. Sanchez Cruz,[130] S. Scarfi,[130] M. Selvaggi,[130] K. Shchelina,[130] P. Silva,[130] P. Sphicas,[130,eee] A. G. Stahl Leiton,[130] A. Steen,[130] S. Summers,[130] D. Treille,[130] P. Tropea,[130] E. Vernazza,[130] J. Wanczyk,[130,fff] S. Wuchterl,[130] M. Zarucki,[130] P. Zehetner,[130] P. Zejdl,[130] G. Zevi Della Porta,[130] T. Bevilacqua,[131,ggg] L. Caminada,[131,ggg] W. Erdmann,[131] R. Horisberger,[131] Q. Ingram,[131] H. C. Kaestli,[131] D. Kotlinski,[131] C. Lange,[131] U. Langenegger,[131] A. Nigamova,[131] L. Noehte,[131,ggg] T. Rohe,[131] A. Samalan,[131] T. K. Aarrestad,[132] M. Backhaus,[132] G. Bonomelli,[132] C. Cazzaniga,[132] K. Datta,[132] P. De Bryas Dexmiers D'Archiacchiac,[132,fff] A. De Cosa,[132] G. Dissertori,[132] M. Dittmar,[132] M. Donegà,[132] F. Glessgen,[132] C. Grab,[132] N. Härringer,[132] T. G. Harte,[132] W. Lustermann,[132] M. Malucchi,[132] R. A. Manzoni,[132] L. Marchese,[132] A. Mascellani,[132,fff] F. Nessi-Tedaldi,[132] F. Pauss,[132] V. Perovic,[132] B. Ristic,[132] R. Seidita,[132] J. Steggemann,[132,fff] A. Tarabini,[132] D. Valsecchi,[132] R. Wallny,[132] C. Amsler,[133,hhh] P. Bärtschi,[133] F. Bilandzija,[133] M. F. Canelli,[133] G. Celotto,[133] A. Jofrehei,[133] B. Kilminster,[133] T. H. Kwok,[133] S. Leontsinis,[133] V. Lukashenko,[133] A. Macchiolo,[133] F. Meng,[133] M. Missiroli,[133] J. Motta,[133] P. Robmann,[133] E. Shokr,[133] F. Stäger,[133] R. Tramontano,[133] P. Viscone,[133] D. Bhowmik,[134] C. M. Kuo,[134] P. K. Rout,[134] S. Taj,[134] P. C. Tiwari,[134,jj] L. Ceard,[135] K. F. Chen,[135] Z. g. Chen,[135] A. De Iorio,[135] W.-S. Hou,[135] T. h. Hsu,[135] Y. w. Kao,[135] S. Karmakar,[135] G. Kole,[135] Y. y. Li,[135] R.-S. Lu,[135] E. Paganis,[135] X. f. Su,[135] J. Thomas-Wilsker,[135] L. s. Tsai,[135] D. Tsionou,[135] H. y. Wu,[135] E. Yazgan,[135] C. Asawatangtrakuldee,[136] N. Srimanobhas,[136] Y. Maghrbi,[137] D. Agyel,[138] F. Dolek,[138] I. Dumanoglu,[138,iii] Y. Guler,[138,jjj] E. Gurpinar Guler,[138,jjj] C. Isik,[138]

O. Kara,[138,kkk] A. Kayis Topaksu,[138] Y. Komurcu,[138] G. Onengut,[138] K. Ozdemir,[138,lll] B. Tali,[138,mmm] U. G. Tok,[138] E. Uslan,[138] I. S. Zorbakir,[138] S. Sen,[139] M. Yalvac,[140,nnn] B. Akgun,[141] I. O. Atakisi,[141,ooo] E. Gülmez,[141] M. Kaya,[141,ppp] O. Kaya,[141,qqq] M. A. Sarkisla,[141,rrr] S. Tekten,[141,sss] D. Boncukcu,[142] A. Cakir,[142] K. Cankocak,[142,iii,ttt] B. Hacisahinoglu,[143] I. Hos,[143,uuu] B. Kaynak,[143] S. Ozkorucuklu,[143] O. Potok,[143] H. Sert,[143] C. Simsek,[143] C. Zorbilmez,[143] S. Cerci,[144] C. Dozen,[144,vvv] B. Isildak,[144] E. Simsek,[144] D. Sunar Cerci,[144] T. Yetkin,[144,vvv] A. Boyaryntsev,[145] O. Dadazhanova,[145] B. Grynyov,[145] L. Levchuk,[146] J. J. Brooke,[147] A. Bundock,[147] F. Bury,[147] E. Clement,[147] D. Cussans,[147] D. Dharmender,[147] H. Flacher,[147] J. Goldstein,[147] H. F. Heath,[147] M.-L. Holmberg,[147] L. Kreczko,[147] S. Paramesvaran,[147] L. Robertshaw,[147] M. S. Sanjrani,[147,mm] J. Segal,[147] V. J. Smith,[147] A. H. Ball,[148] K. W. Bell,[148] A. Belyaev,[148,www] C. Brew,[148] R. M. Brown,[148] D. J. A. Cockerill,[148] A. Elliot,[148] K. V. Ellis,[148] J. Gajownik,[148] K. Harder,[148] S. Harper,[148] J. Linacre,[148] K. Manolopoulos,[148] M. Moallemi,[148] D. M. Newbold,[148] E. Olaiya,[148] D. Petyt,[148] T. Reis,[148] A. R. Sahasransu,[148] G. Salvi,[148] T. Schuh,[148] C. H. Shepherd-Themistocleous,[148] I. R. Tomalin,[148] K. C. Whalen,[148] T. Williams,[148] I. Andreou,[149] R. Bainbridge,[149] P. Bloch,[149] O. Buchmuller,[149] C. A. Carrillo Montoya,[149] D. Colling,[149] I. Das,[149] P. Dauncey,[149] G. Davies,[149] M. Della Negra,[149] S. Fayer,[149] G. Fedi,[149] G. Hall,[149] H. R. Hoorani,[149] A. Howard,[149] G. Iles,[149] C. R. Knight,[149] P. Krueper,[149] J. Langford,[149] K. H. Law,[149] J. León Holgado,[149] L. Lyons,[149] A.-M. Magnan,[149] B. Maier,[149] S. Mallios,[149] A. Mastronikolis,[149] M. Mieskolainen,[149] J. Nash,[149,xxx] M. Pesaresi,[149] P. B. Pradeep,[149] B. C. Radburn-Smith,[149] A. Richards,[149] A. Rose,[149] L. Russell,[149] K. Savva,[149] C. Seez,[149] R. Shukla,[149] A. Tapper,[149] K. Uchida,[149] G. P. Uttley,[149] T. Virdee,[149,aa] M. Vojinovic,[149] N. Wardle,[149] D. Winterbottom,[149] J. E. Cole,[150] A. Khan,[150] P. Kyberd,[150] I. D. Reid,[150] S. Abdullin,[151] A. Brinkerhoff,[151] E. Collins,[151] M. R. Darwish,[151] J. Dittmann,[151] K. Hatakeyama,[151] V. Hegde,[151] J. Hiltbrand,[151] B. McMaster,[151] J. Samudio,[151] S. Sawant,[151] C. Sutantawibul,[151] J. Wilson,[151] J. M. Hogan,[152] R. Bartek,[153] A. Dominguez,[153] S. Raj,[153] B. Sahu,[153,ii] A. E. Simsek,[153] S. S. Yu,[153] B. Bam,[154] A. Buchot Perraguin,[154] S. Campbell,[154] R. Chudasama,[154] S. I. Cooper,[154] C. Crovella,[154] G. Fidalgo,[154] S. V. Gleyzer,[154] A. Khukhunaishvili,[154] K. Matchev,[154] E. Pearson,[154] P. Rumerio,[154,yyy] E. Usai,[154] R. Yi,[154] S. Cholak,[155] G. De Castro,[155] Z. Demiragli,[155] C. Erice,[155] C. Fangmeier,[155] C. Fernandez Madrazo,[155] J. Fulcher,[155] F. Golf,[155] S. Jeon,[155] J. O'Cain,[155] I. Reed,[155] J. Rohlf,[155] K. Salyer,[155] D. Sperka,[155] D. Spitzbart,[155] I. Suarez,[155] A. Tsatsos,[155] E. Wurtz,[155] A. G. Zecchinelli,[155] G. Barone,[156] G. Benelli,[156] D. Cutts,[156] S. Ellis,[156] L. Gouskos,[156] M. Hadley,[156] U. Heintz,[156] K. W. Ho,[156] T. Kwon,[156] L. Lambrecht,[156] G. Landsberg,[156] K. T. Lau,[156] J. Luo,[156] S. Mondal,[156] J. Roloff,[156] T. Russell,[156] S. Sagir,[156,zzz] X. Shen,[156] M. Stamenkovic,[156] N. Venkatasubramanian,[156] S. Abbott,[157] S. Baradia,[157] B. Barton,[157] R. Breedon,[157] H. Cai,[157] M. Calderon De La Barca Sanchez,[157] E. Cannaert,[157] M. Chertok,[157] M. Citron,[157] J. Conway,[157] P. T. Cox,[157] F. Eble,[157] R. Erbacher,[157] O. Kukral,[157] G. Mocellin,[157] S. Ostrom,[157] I. Salazar Segovia,[157] J. S. Tafoya Vargas,[157] W. Wei,[157] S. Yoo,[157] K. Adamidis,[158] M. Bachtis,[158] D. Campos,[158] R. Cousins,[158] S. Crossley,[158] G. Flores Avila,[158] J. Hauser,[158] M. Ignatenko,[158] M. A. Iqbal,[158] T. Lam,[158] Y. f. Lo,[158] E. Manca,[158] A. Nunez Del Prado,[158] D. Saltzberg,[158] V. Valuev,[158] R. Clare,[159] J. W. Gary,[159] G. Hanson,[159] A. Aportela,[160] A. Arora,[160] J. G. Branson,[160] S. Cittolin,[160] S. Cooperstein,[160] B. D'Anzi,[160] D. Diaz,[160] J. Duarte,[160] L. Giannini,[160] Y. Gu,[160] J. Guiang,[160] V. Krutelyov,[160] R. Lee,[160] J. Letts,[160] H. Li,[160] M. Masciovecchio,[160] F. Mokhtar,[160] S. Mukherjee,[160] M. Pieri,[160] D. Primosch,[160] M. Quinnan,[160] V. Sharma,[160] M. Tadel,[160] E. Vourliotis,[160] F. Würthwein,[160] A. Yagil,[160] Z. Zhao,[160] A. Barzdukas,[161] L. Brennan,[161] C. Campagnari,[161] S. Carron Montero,[161,aaaa] K. Downham,[161] C. Grieco,[161] M. M. Hussain,[161] J. Incandela,[161] M. W. K. Lai,[161] A. J. Li,[161] P. Masterson,[161] J. Richman,[161] S. N. Santpur,[161] R. Schmitz,[161] D. Stuart,[161] T. Á. Vámi,[161] X. Yan,[161] D. Zhang,[161] A. Albert,[162] S. Bhattacharya,[162] A. Bornheim,[162] O. Cerri,[162] R. Kansal,[162] J. Mao,[162] H. B. Newman,[162] G. Reales Gutiérrez,[162] T. Sievert,[162] M. Spiropulu,[162] J. R. Vlimant,[162] R. A. Wynne,[162] S. Xie,[162] J. Alison,[163] S. An,[163] M. Cremonesi,[163] V. Dutta,[163] E. Y. Ertorer,[163] T. Ferguson,[163] T. A. Gómez Espinosa,[163] A. Harilal,[163] A. Kallil Tharayil,[163] M. Kanemura,[163] C. Liu,[163] M. Marchegiani,[163] P. Meiring,[163] S. Murthy,[163] P. Palit,[163] K. Park,[163] M. Paulini,[163] A. Roberts,[163] A. Sanchez,[163] W. Terrill,[163] J. P. Cumalat,[164] W. T. Ford,[164] A. Hart,[164] S. Kwan,[164] J. Pearkes,[164] C. Savard,[164] N. Schonbeck,[164] K. Stenson,[164] K. A. Ulmer,[164] S. R. Wagner,[164] N. Zipper,[164] D. Zuolo,[164] J. Alexander,[165] X. Chen,[165]

J. Dickinson,[165] A. Duquette,[165] J. Fan,[165] X. Fan,[165] J. Grassi,[165] S. Hogan,[165] P. Kotamnives,[165] J. Monroy,[165] G. Niendorf,[165] M. Oshiro,[165] J. R. Patterson,[165] A. Ryd,[165] J. Thom,[165] P. Wittich,[165] R. Zou,[165] L. Zygala,[165] M. Albrow,[166] M. Alyari,[166] O. Amram,[166] G. Apollinari,[166] A. Apresyan,[166] L. A. T. Bauerdick,[166] D. Berry,[166] J. Berryhill,[166] P. C. Bhat,[166] K. Burkett,[166] J. N. Butler,[166] A. Canepa,[166] G. B. Cerati,[166] H. W. K. Cheung,[166] F. Chlebana,[166] C. Cosby,[166] G. Cummings,[166] I. Dutta,[166] V. D. Elvira,[166] J. Freeman,[166] A. Gandrakota,[166] Z. Gecse,[166] L. Gray,[166] D. Green,[166] A. Grummer,[166] S. Grünendahl,[166] D. Guerrero,[166] O. Gutsche,[166] R. M. Harris,[166] J. Hirschauer,[166] V. Innocente,[166] B. Jayatilaka,[166] S. Jindariani,[166] M. Johnson,[166] U. Joshi,[166] B. Klima,[166] S. Lammel,[166] C. Lee,[166] D. Lincoln,[166] R. Lipton,[166] T. Liu,[166] K. Maeshima,[166] D. Mason,[166] P. McBride,[166] P. Merkel,[166] S. Mrenna,[166] S. Nahn,[166] J. Ngadiuba,[166] D. Noonan,[166] S. Norberg,[166] V. Papadimitriou,[166] N. Pastika,[166] K. Pedro,[166] C. Pena,[166,bbbb] C. E. Perez Lara,[166] F. Ravera,[166] A. Reinsvold Hall,[166,cccc] L. Ristori,[166] M. Safdari,[166] E. Sexton-Kennedy,[166] N. Smith,[166] A. Soha,[166] L. Spiegel,[166] S. Stoynev,[166] J. Strait,[166] L. Taylor,[166] S. Tkaczyk,[166] N. V. Tran,[166] L. Uplegger,[166] E. W. Vaandering,[166] C. Wang,[166] I. Zoi,[166] C. Aruta,[167] P. Avery,[167] D. Bourilkov,[167] P. Chang,[167] V. Cherepanov,[167] R. D. Field,[167] C. Huh,[167] E. Koenig,[167] M. Kolosova,[167] J. Konigsberg,[167] A. Korytov,[167] G. Mitselmakher,[167] K. Mohrman,[167] A. Muthirakalayil Madhu,[167] N. Rawal,[167] S. Rosenzweig,[167] V. Sulimov,[167] Y. Takahashi,[167] J. Wang,[167] T. Adams,[168] A. Al Kadhim,[168] A. Askew,[168] S. Bower,[168] R. Goff,[168] R. Hashmi,[168] A. Hassani,[168] R. S. Kim,[168] T. Kolberg,[168] G. Martinez,[168] M. Mazza,[168] H. Prosper,[168] P. R. Prova,[168] R. Yohay,[168] B. Alsufyani,[169] S. Butalla,[169] S. Das,[169] M. Hohlmann,[169] M. Lavinsky,[169] E. Yanes,[169] M. R. Adams,[170] N. Barnett,[170] A. Baty,[170] C. Bennett,[170] R. Cavanaugh,[170] R. Escobar Franco,[170] O. Evdokimov,[170] C. E. Gerber,[170] H. Gupta,[170] M. Hawksworth,[170] A. Hingrajiya,[170] D. J. Hofman,[170] Z. Huang,[170] J. h. Lee,[170] C. Mills,[170] S. Nanda,[170] G. Nigmatkulov,[170] B. Ozek,[170] T. Phan,[170] D. Pilipovic,[170] R. Pradhan,[170] E. Prifti,[170] P. Roy,[170] T. Roy,[170] D. Shekar,[170] N. Singh,[170] A. Thielen,[170] M. B. Tonjes,[170] N. Varelas,[170] M. A. Wadud,[170] J. Yoo,[170] M. Alhusseini,[171] D. Blend,[171] K. Dilsiz,[171,dddd] O. K. Köseyan,[171] A. Mestvirishvili,[171,eeee] O. Neogi,[171] H. Ogul,[171,ffff] Y. Onel,[171] A. Penzo,[171] C. Snyder,[171] E. Tiras,[171,gggg] B. Blumenfeld,[172] J. Davis,[172] A. V. Gritsan,[172] L. Kang,[172] S. Kyriacou,[172] P. Maksimovic,[172] M. Roguljic,[172] S. Sekhar,[172] M. V. Srivastav,[172] M. Swartz,[172] A. Abreu,[173] L. F. Alcerro Alcerro,[173] J. Anguiano,[173] S. Arteaga Escatel,[173] P. Baringer,[173] A. Bean,[173] R. Bhattacharya,[173] Z. Flowers,[173] D. Grove,[173] J. King,[173] G. Krintiras,[173] M. Lazarovits,[173] C. Le Mahieu,[173] J. Marquez,[173] M. Murray,[173] M. Nickel,[173] S. Popescu,[173,hhhh] C. Rogan,[173] C. Royon,[173] S. Rudrabhatla,[173] S. Sanders,[173] C. Smith,[173] G. Wilson,[173] B. Allmond,[174] N. Islam,[174] A. Ivanov,[174] K. Kaadze,[174] Y. Maravin,[174] J. Natoli,[174] G. G. Reddy,[174] D. Roy,[174] G. Sorrentino,[174] A. Baden,[175] A. Belloni,[175] J. Bistany-riebman,[175] S. C. Eno,[175] N. J. Hadley,[175] S. Jabeen,[175] R. G. Kellogg,[175] T. Koeth,[175] B. Kronheim,[175] S. Lascio,[175] P. Major,[175] A. C. Mignerey,[175] C. Palmer,[175] C. Papageorgakis,[175] M. M. Paranjpe,[175] E. Popova,[175,iiii] A. Shevelev,[175] L. Zhang,[175] C. Baldenegro Barrera,[176] H. Bossi,[176] S. Bright-Thonney,[176] I. A. Cali,[176] Y. c. Chen,[176] P. c. Chou,[176] M. D'Alfonso,[176] J. Eysermans,[176] C. Freer,[176] G. Gomez-Ceballos,[176] M. Goncharov,[176] G. Grosso,[176] P. Harris,[176] D. Hoang,[176] G. M. Innocenti,[176] K. Ivanov,[176] D. Kovalskyi,[176] J. Krupa,[176] L. Lavezzo,[176] Y.-J. Lee,[176] K. Long,[176] C. Mcginn,[176] A. Novak,[176] M. I. Park,[176] C. Paus,[176] C. Reissel,[176] C. Roland,[176] G. Roland,[176] S. Rothman,[176] T. a. Sheng,[176] G. S. F. Stephans,[176] D. Walter,[176] J. Wang,[176] Z. Wang,[176] B. Wyslouch,[176] T. J. Yang,[176] A. Alpana,[177] B. Crossman,[177] W. J. Jackson,[177] C. Kapsiak,[177] M. Krohn,[177] D. Mahon,[177] J. Mans,[177] B. Marzocchi,[177] R. Rusack,[177] O. Sancar,[177] R. Saradhy,[177] N. Strobbe,[177] K. Bloom,[178] D. R. Claes,[178] G. Haza,[178] J. Hossain,[178] C. Joo,[178] I. Kravchenko,[178] K. H. M. Kwok,[178] A. Rohilla,[178] J. E. Siado,[178] W. Tabb,[178] A. Vagnerini,[178] A. Wightman,[178] F. Yan,[178] H. Bandyopadhyay,[179] L. Hay,[179] H. w. Hsia,[179] I. Iashvili,[179] A. Kalogeropoulos,[179] A. Kharchilava,[179] A. Mandal,[179] M. Morris,[179] D. Nguyen,[179] S. Rappoccio,[179] H. Rejeb Sfar,[179] A. Williams,[179] D. Yu,[179] A. Aarif,[180] G. Alverson,[180] E. Barberis,[180] J. Bonilla,[180] B. Bylsma,[180] M. Campana,[180] J. Dervan,[180] Y. Haddad,[180] Y. Han,[180] I. Israr,[180] A. Krishna,[180] M. Lu,[180] N. Manganelli,[180] R. Mccarthy,[180] D. M. Morse,[180] T. Orimoto,[180] L. Skinnari,[180] C. S. Thoreson,[180] E. Tsai,[180] D. Wood,[180] S. Dittmer,[181] K. A. Hahn,[181] M. Mcginnis,[181] Y. Miao,[181] D. G. Monk,[181] M. H. Schmitt,[181] A. Taliercio,[181] M. Velasco,[181] J. Wang,[181] G. Agarwal,[182] R. Band,[182] R. Bucci,[182] S. Castells,[182] A. Das,[182] A. Datta,[182] A. Ehnis,[182]

R. Goldouzian,[182] M. Hildreth,[182] K. Hurtado Anampa,[182] T. Ivanov,[182] C. Jessop,[182] A. Karneyeu,[182] K. Lannon,[182] J. Lawrence,[182] N. Loukas,[182] L. Lutton,[182] J. Mariano,[182] N. Marinelli,[182] T. McCauley,[182] C. Mcgrady,[182] C. Moore,[182] Y. Musienko,[182,iiii] H. Nelson,[182] M. Osherson,[182] A. Piccinelli,[182] R. Ruchti,[182] A. Townsend,[182] Y. Wan,[182] M. Wayne,[182] H. Yockey,[182] A. Basnet,[183] M. Carrigan,[183] R. De Los Santos,[183] L. S. Durkin,[183] C. Hill,[183] M. Joyce,[183] D. A. Wenzl,[183] B. L. Winer,[183] B. R. Yates,[183] H. Bouchamaoui,[184] G. Dezoort,[184] P. Elmer,[184] A. Frankenthal,[184] M. Galli,[184] B. Greenberg,[184] N. Haubrich,[184] K. Kennedy,[184] G. Kopp,[184] Y. Lai,[184] D. Lange,[184] A. Loeliger,[184] D. Marlow,[184] I. Ojalvo,[184] J. Olsen,[184] F. Simpson,[184] D. Stickland,[184] C. Tully,[184] S. Malik,[185] R. Sharma,[185] S. Chandra,[186] A. Gu,[186] L. Gutay,[186] M. Huwiler,[186] M. Jones,[186] A. W. Jung,[186] D. Kondratyev,[186] J. Li,[186] M. Liu,[186] G. Negro,[186] N. Neumeister,[186] G. Paspalaki,[186] S. Piperov,[186] N. R. Saha,[186] J. F. Schulte,[186] F. Wang,[186] A. Wildridge,[186] W. Xie,[186] Y. Yao,[186] Y. Zhong,[186] N. Parashar,[187] A. Pathak,[187] E. Shumka,[187] D. Acosta,[188] A. Agrawal,[188] C. Arbour,[188] T. Carnahan,[188] P. Das,[188] K. M. Ecklund,[188] F. J. M. Geurts,[188] T. Huang,[188] I. Krommydas,[188] N. Lewis,[188] W. Li,[188] J. Lin,[188] O. Miguel Colin,[188] B. P. Padley,[188] R. Redjimi,[188] J. Rotter,[188] C. Vico Villalba,[188] M. Wulansatiti,[188] E. Yigitbasi,[188] Y. Zhang,[188] O. Bessidskaia Bylund,[189] A. Bodek,[189] P. de Barbaro,[189,a] R. Demina,[189] A. Garcia-Bellido,[189] H. S. Hare,[189] O. Hindrichs,[189] N. Parmar,[189] P. Parygin,[189,iiii] H. Seo,[189] R. Taus,[189] B. Chiarito,[190] J. P. Chou,[190] S. V. Clark,[190] S. Donnelly,[190] D. Gadkari,[190] Y. Gershtein,[190] E. Halkiadakis,[190] C. Houghton,[190] D. Jaroslawski,[190] A. Kobert,[190] I. Laflotte,[190] A. Lath,[190] J. Martins,[190] M. Perez Prada,[190] B. Rand,[190] J. Reichert,[190] P. Saha,[190] S. Salur,[190] S. Schnetzer,[190] S. Somalwar,[190] R. Stone,[190] S. A. Thayil,[190] S. Thomas,[190] J. Vora,[190] D. Ally,[191] A. G. Delannoy,[191] S. Fiorendi,[191] J. Harris,[191] T. Holmes,[191] A. R. Kanuganti,[191] N. Karunarathna,[191] J. Lawless,[191] L. Lee,[191] E. Nibigira,[191] B. Skipworth,[191] S. Spanier,[191] D. Aebi,[192] M. Ahmad,[192] T. Akhter,[192] K. Androsov,[192] A. Bolshov,[192] O. Bouhali,[192,jjjj] A. Cagnotta,[192] V. D'Amante,[192] R. Eusebi,[192] P. Flanagan,[192] J. Gilmore,[192] Y. Guo,[192] T. Kamon,[192] S. Luo,[192] R. Mueller,[192] A. Safonov,[192] N. Akchurin,[193] J. Damgov,[193] Y. Feng,[193] N. Gogate,[193] W. Jin,[193] Y. Kazhykarim,[193] K. Lamichhane,[193] S. W. Lee,[193] C. Madrid,[193] A. Mankel,[193] T. Peltola,[193] I. Volobouev,[193] E. Appelt,[194] Y. Chen,[194] S. Greene,[194] A. Gurrola,[194] W. Johns,[194] R. Kunnawalkam Elayavalli,[194] A. Melo,[194] D. Rathjens,[194] F. Romeo,[194] P. Sheldon,[194] S. Tuo,[194] J. Velkovska,[194] J. Viinikainen,[194] J. Zhang,[194] B. Cardwell,[195] H. Chung,[195] B. Cox,[195] J. Hakala,[195] G. Hamilton Ilha Machado,[195] R. Hirosky,[195] M. Jose,[195] A. Ledovskoy,[195] C. Mantilla,[195] C. Neu,[195] C. Ramón Álvarez,[195] Z. Wu,[195] S. Bhattacharya,[196] P. E. Karchin,[196] A. Aravind,[197] S. Banerjee,[197] K. Black,[197] T. Bose,[197] E. Chavez,[197] S. Dasu,[197] P. Everaerts,[197] C. Galloni,[197] H. He,[197] M. Herndon,[197] A. Herve,[197] C. K. Koraka,[197] S. Lomte,[197] R. Loveless,[197] A. Mallampalli,[197] A. Mohammadi,[197] S. Mondal,[197] T. Nelson,[197] G. Parida,[197] L. Pétré,[197] D. Pinna,[197] A. Savin,[197] V. Shang,[197] V. Sharma,[197] W. H. Smith,[197] D. Teague,[197] H. F. Tsoi,[197] W. Vetens,[197] A. Warden,[197] S. Afanasiev,[198] V. Alexakhin,[198] Yu. Andreev,[198] T. Aushev,[198] D. Budkouski,[198] R. Chistov,[198] M. Danilov,[198] T. Dimova,[198] A. Ershov,[198] S. Gninenko,[198] I. Gorbunov,[198] A. Gribushin,[198] A. Kamenev,[198] V. Karjavine,[198] M. Kirsanov,[198] O. Kodolova,[198,kkkk] V. Korenkov,[198] I. Korsakov,[198] A. Kozyrev,[198] N. Krasnikov,[198] A. Lanev,[198] A. Malakhov,[198] V. Matveev,[198] A. Nikitenko,[198,llll,kkkk] V. Palichik,[198] V. Perelygin,[198] S. Polikarpov,[198] O. Radchenko,[198] M. Savina,[198] V. Shalaev,[198] S. Shmatov,[198] S. Shulha,[198] Y. Skovpen,[198] K. Slizhevskiy,[198] V. Smirnov,[198] O. Teryaev,[198] I. Tlisova,[198] A. Toropin,[198] N. Voytishin,[198] A. Zarubin,[198] I. Zhizhin,[198] L. Dudko,[199] V. Kim,[199,iiii] V. Murzin,[199] V. Oreshkin,[199] and D. Sosnov[199]

(CMS Collaboration)

[1]*Yerevan Physics Institute, Yerevan, Armenia*
[2]*Institut für Hochenergiephysik, Vienna, Austria*
[3]*Universiteit Antwerpen, Antwerpen, Belgium*
[4]*Vrije Universiteit Brussel, Brussel, Belgium*
[5]*Université Libre de Bruxelles, Bruxelles, Belgium*
[6]*Ghent University, Ghent, Belgium*
[7]*Université Catholique de Louvain, Louvain-la-Neuve, Belgium*

[8]*Centro Brasileiro de Pesquisas Fisicas, Rio de Janeiro, Brazil*
[9]*Universidade do Estado do Rio de Janeiro, Rio de Janeiro, Brazil*
[10]*Universidade Estadual Paulista, Universidade Federal do ABC, São Paulo, Brazil*
[11]*Institute for Nuclear Research and Nuclear Energy, Bulgarian Academy of Sciences, Sofia, Bulgaria*
[12]*University of Sofia, Sofia, Bulgaria*
[13]*Instituto De Alta Investigación, Universidad de Tarapacá, Casilla 7 D, Arica, Chile*
[14]*Universidad Tecnica Federico Santa Maria, Valparaiso, Chile*
[15]*Beihang University, Beijing, China*
[16]*Department of Physics, Tsinghua University, Beijing, China*
[17]*Institute of High Energy Physics, Beijing, China*
[18]*State Key Laboratory of Nuclear Physics and Technology, Peking University, Beijing, China*
[19]*State Key Laboratory of Nuclear Physics and Technology, Institute of Quantum Matter, South China Normal University, Guangzhou, China*
[20]*Sun Yat-Sen University, Guangzhou, China*
[21]*University of Science and Technology of China, Hefei, China*
[22]*Nanjing Normal University, Nanjing, China*
[23]*Institute of Modern Physics and Key Laboratory of Nuclear Physics and Ion-beam Application (MOE)—Fudan University, Shanghai, China*
[24]*Zhejiang University, Hangzhou, Zhejiang, China*
[25]*Universidad de Los Andes, Bogota, Colombia*
[26]*Universidad de Antioquia, Medellin, Colombia*
[27]*University of Split, Faculty of Electrical Engineering, Mechanical Engineering and Naval Architecture, Split, Croatia*
[28]*University of Split, Faculty of Science, Split, Croatia*
[29]*Institute Rudjer Boskovic, Zagreb, Croatia*
[30]*University of Cyprus, Nicosia, Cyprus*
[31]*Charles University, Prague, Czech Republic*
[32]*Escuela Politecnica Nacional, Quito, Ecuador*
[33]*Universidad San Francisco de Quito, Quito, Ecuador*
[34]*Academy of Scientific Research and Technology of the Arab Republic of Egypt, Egyptian Network of High Energy Physics, Cairo, Egypt*
[35]*Center for High Energy Physics (CHEP-FU), Fayoum University, El-Fayoum, Egypt*
[36]*National Institute of Chemical Physics and Biophysics, Tallinn, Estonia*
[37]*Department of Physics, University of Helsinki, Helsinki, Finland*
[38]*Helsinki Institute of Physics, Helsinki, Finland*
[39]*Lappeenranta-Lahti University of Technology, Lappeenranta, Finland*
[40]*IRFU, CEA, Université Paris-Saclay, Gif-sur-Yvette, France*
[41]*Laboratoire Leprince-Ringuet, CNRS/IN2P3, Ecole Polytechnique, Institut Polytechnique de Paris, Palaiseau, France*
[42]*Université de Strasbourg, CNRS, IPHC UMR 7178, Strasbourg, France*
[43]*Centre de Calcul de l'Institut National de Physique Nucleaire et de Physique des Particules, CNRS/IN2P3, Villeurbanne, France*
[44]*Institut de Physique des 2 Infinis de Lyon (IP2I), Villeurbanne, France*
[45]*Georgian Technical University, Tbilisi, Georgia*
[46]*RWTH Aachen University, I. Physikalisches Institut, Aachen, Germany*
[47]*RWTH Aachen University, III. Physikalisches Institut A, Aachen, Germany*
[48]*RWTH Aachen University, III. Physikalisches Institut B, Aachen, Germany*
[49]*Deutsches Elektronen-Synchrotron, Hamburg, Germany*
[50]*University of Hamburg, Hamburg, Germany*
[51]*Karlsruher Institut fuer Technologie, Karlsruhe, Germany*
[52]*Institute of Nuclear and Particle Physics (INPP), NCSR Demokritos, Aghia Paraskevi, Greece*
[53]*National and Kapodistrian University of Athens, Athens, Greece*
[54]*National Technical University of Athens, Athens, Greece*
[55]*University of Ioánnina, Ioánnina, Greece*
[56]*HUN-REN Wigner Research Centre for Physics, Budapest, Hungary*
[57]*MTA-ELTE Lendület CMS Particle and Nuclear Physics Group, Eötvös Loránd University, Budapest, Hungary*
[58]*Faculty of Informatics, University of Debrecen, Debrecen, Hungary*
[59]*HUN-REN ATOMKI—Institute of Nuclear Research, Debrecen, Hungary*
[60]*Karoly Robert Campus, MATE Institute of Technology, Gyongyos, Hungary*

[61]IIT Bhubaneswar, Bhubaneswar, India
[62]Panjab University, Chandigarh, India
[63]University of Delhi, Delhi, India
[64]Indian Institute of Technology Mandi (IIT-Mandi), Himachal Pradesh, India
[65]University of Hyderabad, Hyderabad, India
[66]Indian Institute of Technology Kanpur, Kanpur, India
[67]Saha Institute of Nuclear Physics, HBNI, Kolkata, India
[68]Indian Institute of Technology Madras, Madras, India
[69]IISER Mohali, India, Mohali, India
[70]Tata Institute of Fundamental Research-A, Mumbai, India
[71]Tata Institute of Fundamental Research-B, Mumbai, India
[72]National Institute of Science Education and Research, An OCC of Homi Bhabha National Institute, Bhubaneswar, Odisha, India
[73]Indian Institute of Science Education and Research (IISER), Pune, India
[74]Indian Institute of Technology Hyderabad, Telangana, India
[75]Isfahan University of Technology, Isfahan, Iran
[76]Institute for Research in Fundamental Sciences (IPM), Tehran, Iran
[77]University College Dublin, Dublin, Ireland
[78a]INFN Sezione di Bari, Bari, Italy
[78b]Università di Bari , Bari, Italy
[78c]Politecnico di Bari, Bari, Italy
[79a]INFN Sezione di Bologna, Bologna, Italy
[79b]Università di Bologna , Bologna, Italy
[80a]INFN Sezione di Catania, Catania, Italy
[80b]Università di Catania , Catania, Italy
[81a]INFN Sezione di Firenze, Firenze, Italy
[81b]Università di Firenze , Firenze, Italy
[82]INFN Laboratori Nazionali di Frascati, Frascati, Italy
[83a]INFN Sezione di Genova, Genova, Italy
[83b]Università di Genova , Genova, Italy
[84a]INFN Sezione di Milano-Bicocca, Milano, Italy
[84b]Università di Milano-Bicocca , Milano, Italy
[85a]INFN Sezione di Napoli, Napoli, Italy
[85b]Università di Napoli 'Federico II' , Napoli, Italy
[85c]Università della Basilicata , Potenza, Italy
[85d]Scuola Superiore Meridionale (SSM), Napoli, Italy
[86a]INFN Sezione di Padova, Padova, Italy
[86b]Università di Padova , Padova, Italy
[86c]Universita degli Studi di Cagliari , Cagliari, Italy
[87a]INFN Sezione di Pavia, Pavia, Italy
[87b]Università di Pavia , Pavia, Italy
[88a]INFN Sezione di Perugia, Perugia, Italy
[88b]Università di Perugia , Perugia, Italy
[89a]INFN Sezione di Pisa, Pisa, Italy
[89b]Università di Pisa , Pisa, Italy
[89c]Scuola Normale Superiore di Pisa, Pisa, Italy
[89d]Università di Siena , Siena, Italy
[90a]INFN Sezione di Roma, Roma, Italy
[90b]Sapienza Università di Roma , Roma, Italy
[91a]INFN Sezione di Torino, Torino, Italy
[91b]Università di Torino , Torino, Italy
[91c]Università del Piemonte Orientale , Novara, Italy
[92a]INFN Sezione di Trieste, Trieste, Italy
[92b]Università di Trieste , Trieste, Italy
[93]Kyungpook National University, Daegu, Korea
[94]Department of Mathematics and Physics—GWNU, Gangneung, Korea
[95]Chonnam National University, Institute for Universe and Elementary Particles, Kwangju, Korea
[96]Hanyang University, Seoul, Korea
[97]Korea University, Seoul, Korea
[98]Kyung Hee University, Department of Physics, Seoul, Korea

[99]*Sejong University, Seoul, Korea*
[100]*Seoul National University, Seoul, Korea*
[101]*University of Seoul, Seoul, Korea*
[102]*Yonsei University, Department of Physics, Seoul, Korea*
[103]*Sungkyunkwan University, Suwon, Korea*
[104]*College of Engineering and Technology, American University of the Middle East (AUM), Dasman, Kuwait*
[105]*Kuwait University—College of Science—Department of Physics, Safat, Kuwait*
[106]*Riga Technical University, Riga, Latvia*
[107]*University of Latvia (LU), Riga, Latvia*
[108]*Vilnius University, Vilnius, Lithuania*
[109]*National Centre for Particle Physics, Universiti Malaya, Kuala Lumpur, Malaysia*
[110]*Universidad de Sonora (UNISON), Hermosillo, Mexico*
[111]*Centro de Investigacion y de Estudios Avanzados del IPN, Mexico City, Mexico*
[112]*Universidad Iberoamericana, Mexico City, Mexico*
[113]*Benemerita Universidad Autonoma de Puebla, Puebla, Mexico*
[114]*University of Montenegro, Podgorica, Montenegro*
[115]*University of Canterbury, Christchurch, New Zealand*
[116]*National Centre for Physics, Quaid-I-Azam University, Islamabad, Pakistan*
[117]*AGH University of Krakow, Krakow, Poland*
[118]*National Centre for Nuclear Research, Swierk, Poland*
[119]*Institute of Experimental Physics, Faculty of Physics, University of Warsaw, Warsaw, Poland*
[120]*Warsaw University of Technology, Warsaw, Poland*
[121]*Laboratório de Instrumentação e Física Experimental de Partículas, Lisboa, Portugal*
[122]*Faculty of Physics, University of Belgrade, Belgrade, Serbia*
[123]*VINCA Institute of Nuclear Sciences, University of Belgrade, Belgrade, Serbia*
[124]*Centro de Investigaciones Energéticas Medioambientales y Tecnológicas (CIEMAT), Madrid, Spain*
[125]*Universidad Autónoma de Madrid, Madrid, Spain*
[126]*Universidad de Oviedo, Instituto Universitario de Ciencias y Tecnologías Espaciales de Asturias (ICTEA), Oviedo, Spain*
[127]*Instituto de Física de Cantabria (IFCA), CSIC-Universidad de Cantabria, Santander, Spain*
[128]*University of Colombo, Colombo, Sri Lanka*
[129]*University of Ruhuna, Department of Physics, Matara, Sri Lanka*
[130]*CERN, European Organization for Nuclear Research, Geneva, Switzerland*
[131]*PSI Center for Neutron and Muon Sciences, Villigen, Switzerland*
[132]*ETH Zurich—Institute for Particle Physics and Astrophysics (IPA), Zurich, Switzerland*
[133]*Universität Zürich, Zurich, Switzerland*
[134]*National Central University, Chung-Li, Taiwan*
[135]*National Taiwan University (NTU), Taipei, Taiwan*
[136]*High Energy Physics Research Unit, Department of Physics, Faculty of Science, Chulalongkorn University, Bangkok, Thailand*
[137]*Tunis El Manar University, Tunis, Tunisia*
[138]*Çukurova University, Physics Department, Science and Art Faculty, Adana, Turkey*
[139]*Hacettepe University, Ankara, Turkey*
[140]*Middle East Technical University, Physics Department, Ankara, Turkey*
[141]*Bogazici University, Istanbul, Turkey*
[142]*Istanbul Technical University, Istanbul, Turkey*
[143]*Istanbul University, Istanbul, Turkey*
[144]*Yildiz Technical University, Istanbul, Turkey*
[145]*Institute for Scintillation Materials of National Academy of Science of Ukraine, Kharkiv, Ukraine*
[146]*National Science Centre, Kharkiv Institute of Physics and Technology, Kharkiv, Ukraine*
[147]*University of Bristol, Bristol, United Kingdom*
[148]*Rutherford Appleton Laboratory, Didcot, United Kingdom*
[149]*Imperial College, London, United Kingdom*
[150]*Brunel University, Uxbridge, United Kingdom*
[151]*Baylor University, Waco, Texas, USA*
[152]*Bethel University, St. Paul, Minnesota, USA*
[153]*Catholic University of America, Washington, DC, USA*
[154]*The University of Alabama, Tuscaloosa, Alabama, USA*
[155]*Boston University, Boston, Massachusetts, USA*

[156]Brown University, Providence, Rhode Island, USA
[157]University of California, Davis, Davis, California, USA
[158]University of California, Los Angeles, California, USA
[159]University of California, Riverside, Riverside, California, USA
[160]University of California, San Diego, La Jolla, California, USA
[161]University of California, Santa Barbara—Department of Physics, Santa Barbara, California, USA
[162]California Institute of Technology, Pasadena, California, USA
[163]Carnegie Mellon University, Pittsburgh, Pennsylvania, USA
[164]University of Colorado Boulder, Boulder, Colorado, USA
[165]Cornell University, Ithaca, New York, USA
[166]Fermi National Accelerator Laboratory, Batavia, Illinois, USA
[167]University of Florida, Gainesville, Florida, USA
[168]Florida State University, Tallahassee, Florida, USA
[169]Florida Institute of Technology, Melbourne, Florida, USA
[170]University of Illinois Chicago, Chicago, Illinois, USA
[171]The University of Iowa, Iowa City, Iowa, USA
[172]Johns Hopkins University, Baltimore, Maryland, USA
[173]The University of Kansas, Lawrence, Kansas, USA
[174]Kansas State University, Manhattan, Kansas, USA
[175]University of Maryland, College Park, Maryland, USA
[176]Massachusetts Institute of Technology, Cambridge, Massachusetts, USA
[177]University of Minnesota, Minneapolis, Minnesota, USA
[178]University of Nebraska-Lincoln, Lincoln, Nebraska, USA
[179]State University of New York at Buffalo, Buffalo, New York, USA
[180]Northeastern University, Boston, Massachusetts, USA
[181]Northwestern University, Evanston, Illinois, USA
[182]University of Notre Dame, Notre Dame, Indiana, USA
[183]The Ohio State University, Columbus, Ohio, USA
[184]Princeton University, Princeton, New Jersey, USA
[185]University of Puerto Rico, Mayaguez, Puerto Rico, USA
[186]Purdue University, West Lafayette, Indiana, USA
[187]Purdue University Northwest, Hammond, Indiana, USA
[188]Rice University, Houston, Texas, USA
[189]University of Rochester, Rochester, New York, USA
[190]Rutgers, The State University of New Jersey, Piscataway, New Jersey, USA
[191]University of Tennessee, Knoxville, Tennessee, USA
[192]Texas A&M University, College Station, Texas, USA
[193]Texas Tech University, Lubbock, Texas, USA
[194]Vanderbilt University, Nashville, Tennessee, USA
[195]University of Virginia, Charlottesville, Virginia, USA
[196]Wayne State University, Detroit, Michigan, USA
[197]University of Wisconsin—Madison, Madison, Wisconsin, USA
[198]An institute or international laboratory covered by a cooperation agreement with CERN
[199]An institute formerly covered by a cooperation agreement with CERN

[a]Deceased.
[b]Also at Yerevan State University, Yerevan, Armenia.
[c]Also at TU Wien, Vienna, Austria.
[d]Also at Ghent University, Ghent, Belgium.
[e]Also at FACAMP—Faculdades de Campinas, Sao Paulo, Brazil.
[f]Also at Universidade Estadual de Campinas, Campinas, Brazil.
[g]Also at Federal University of Rio Grande do Sul, Porto Alegre, Brazil.
[h]Also at The University of the State of Amazonas, Manaus, Brazil.
[i]Also at University of Chinese Academy of Sciences, Beijing, China.
[j]Also at University of Chinese Academy of Sciences, Beijing, China.
[k]Also at School of Physics, Zhengzhou University, Zhengzhou, China.
[l]Also at Henan Normal University, Xinxiang, China.
[m]Also at University of Shanghai for Science and Technology, Shanghai, China.
[n]Also at The University of Iowa, Iowa City, Iowa, USA.
[o]Also at Nanjing Normal University, Nanjing, China.

[p]Also at Center for High Energy Physics, Peking University, Beijing, China.
[q]Also at British University in Egypt, Cairo, Egypt.
[r]Also at Cairo University, Cairo, Egypt.
[s]Also at Purdue University, West Lafayette, Indiana, USA.
[t]Also at Université de Haute Alsace, Mulhouse, France.
[u]Also at Another institute or international laboratory covered by a cooperation agreement with CERN.
[v]Also at University of Hamburg, Hamburg, Germany.
[w]Also at RWTH Aachen University, III. Physikalisches Institut A, Aachen, Germany.
[x]Also at Bergische University Wuppertal (BUW), Wuppertal, Germany.
[y]Also at Brandenburg University of Technology, Cottbus, Germany.
[z]Also at Forschungszentrum Jülich, Juelich, Germany.
[aa]Also at CERN, European Organization for Nuclear Research, Geneva, Switzerland.
[bb]Also at HUN-REN ATOMKI—Institute of Nuclear Research, Debrecen, Hungary.
[cc]Also at Universitatea Babes-Bolyai—Facultatea de Fizica, Cluj-Napoca, Romania.
[dd]Also at MTA-ELTE Lendület CMS Particle and Nuclear Physics Group, Eötvös Loránd University, Budapest, Hungary.
[ee]Also at HUN-REN Wigner Research Centre for Physics, Budapest, Hungary.
[ff]Also at Physics Department, Faculty of Science, Assiut University, Assiut, Egypt.
[gg]Also at The University of Kansas, Lawrence, Kansas, USA.
[hh]Also at Punjab Agricultural University, Ludhiana, India.
[ii]Also at University of Hyderabad, Hyderabad, India.
[jj]Also at Indian Institute of Science (IISc), Bangalore, India.
[kk]Also at University of Visva-Bharati, Santiniketan, India.
[ll]Also at Institute of Physics, Bhubaneswar, India.
[mm]Also at Deutsches Elektronen-Synchrotron, Hamburg, Germany.
[nn]Also at Isfahan University of Technology, Isfahan, Iran.
[oo]Also at Sharif University of Technology, Tehran, Iran.
[pp]Also at Department of Physics, University of Science and Technology of Mazandaran, Behshahr, Iran.
[qq]Also at Department of Physics, Faculty of Science, Arak University, ARAK, Iran.
[rr]Also at Helwan University, Cairo, Egypt.
[ss]Also at Italian National Agency for New Technologies, Energy and Sustainable Economic Development, Bologna, Italy.
[tt]Also at Centro Siciliano di Fisica Nucleare e di Struttura Della Materia, Catania, Italy.
[uu]Also at Università degli Studi Guglielmo Marconi, Roma, Italy.
[vv]Also at Scuola Superiore Meridionale, Università di Napoli 'Federico II', Napoli, Italy.
[ww]Also at Fermi National Accelerator Laboratory, Batavia, Illinois, USA.
[xx]Also at Lulea University of Technology, Lulea, Sweden.
[yy]Also at Consiglio Nazionale delle Ricerche—Istituto Officina dei Materiali, Perugia, Italy.
[zz]Also at UPES—University of Petroleum and Energy Studies, Dehradun, India.
[aaa]Also at Institut de Physique des 2 Infinis de Lyon (IP2I), Villeurbanne, France.
[bbb]Also at Department of Applied Physics, Faculty of Science and Technology, Universiti Kebangsaan Malaysia, Bangi, Malaysia.
[ccc]Also at Trincomalee Campus, Eastern University, Sri Lanka, Nilaveli, Sri Lanka.
[ddd]Also at Saegis Campus, Nugegoda, Sri Lanka.
[eee]Also at National and Kapodistrian University of Athens, Athens, Greece.
[fff]Also at Ecole Polytechnique Fédérale Lausanne, Lausanne, Switzerland.
[ggg]Also at Universität Zürich, Zurich, Switzerland.
[hhh]Also at Stefan Meyer Institute for Subatomic Physics, Vienna, Austria.
[iii]Also at Near East University, Research Center of Experimental Health Science, Mersin, Turkey.
[jjj]Also at Konya Technical University, Konya, Turkey.
[kkk]Also at Istanbul Topkapi University, Istanbul, Turkey.
[lll]Also at Izmir Bakircay University, Izmir, Turkey.
[mmm]Also at Adiyaman University, Adiyaman, Turkey.
[nnn]Also at Bozok Universitetesi Rektörlügü, Yozgat, Turkey.
[ooo]Also at Istanbul Sabahattin Zaim University, Istanbul, Turkey.
[ppp]Also at Marmara University, Istanbul, Turkey.
[qqq]Also at Milli Savunma University, Istanbul, Turkey.
[rrr]Also at Informatics and Information Security Research Center, Gebze/Kocaeli, Turkey.
[sss]Also at Kafkas University, Kars, Turkey.
[ttt]Also at Istanbul Okan University, Istanbul, Turkey.
[uuu]Also at Istanbul University—Cerrahpasa, Faculty of Engineering, Istanbul, Turkey.
[vvv]Also at Istinye University, Istanbul, Turkey.
[www]Also at School of Physics and Astronomy, University of Southampton, Southampton, United Kingdom.

[xxx]Also at Monash University, Faculty of Science, Clayton, Australia.
[yyy]Also at Università di Torino, Torino, Italy.
[zzz]Also at Karamanoğlu Mehmetbey University, Karaman, Turkey.
[aaaa]Also at California Lutheran University;, Thousand Oaks, California, USA.
[bbbb]Also at California Institute of Technology, Pasadena, California, USA.
[cccc]Also at United States Naval Academy, Annapolis, Maryland, USA.
[dddd]Also at Bingol University, Bingol, Turkey.
[eeee]Also at Georgian Technical University, Tbilisi, Georgia.
[ffff]Also at Sinop University, Sinop, Turkey.
[gggg]Also at Erciyes University, Kayseri, Turkey.
[hhhh]Also at Horia Hulubei National Institute of Physics and Nuclear Engineering (IFIN-HH), Bucharest, Romania.
[iiii]Also at Another institute formerly covered by a cooperation agreement with CERN.
[jjjj]Also at Hamad Bin Khalifa University (HBKU), Doha, Qatar.
[kkkk]Also at Yerevan Physics Institute, Yerevan, Armenia.
[llll]Also at Imperial College, London, United Kingdom.